OPEN ACCESS
JOURNAL OF ADVANCED DIELECTRICS
Vol. 13, No. 4 (2023) 2341009 (24 pages)

DOI: 10.1142/S2010135X23410096

Ferroelectrets: Heterogenous polymer electrets with high piezoelectric sensitivity for transducers

Xunlin Qiu[*,††,§§], Peng Fang[†,‡‡,§§], Axel Mellinger[‡], Ruy Alberto Pisani Altafim[§], Werner Wirges[¶], Gunnar Gidion[‖] and Dmitry Rychkov[**]

[*]*Shanghai Key Laboratory of Intelligent Sensing and Detection Technology*
School of Mechanical and Power Engineering, East China University of Science and Technology
Shanghai 200237, P. R. China

[†]*CAS Key Laboratory of Human-Machine Intelligence-Synergy Systems*
Shenzhen Institutes of Advanced Technology, Shenzhen 518055, P. R. China

[‡]*Department of Physics, Central Michigan University*
223 Dow Science Complex, Mount Pleasant, MI 48859, USA

[§]*Computer Systems Department, Informatics Center*
Federal University of Paráiba, João Pessoa-PB, Brazil

[¶]*Department of Physics and Astronomy, University of Potsdam*
Potsdam, Brandenburg, Germany

[‖]*Laboratory for Electrical Instrumentation, Department of Microsystems Engineering-IMTEK*
University of Freiburg, Georges-Köhler-Allee 106, Freiburg 79110, Germany

[**]*Technology and Study Center Weissenburg, Deggendorf Institute of Technology*
Weissenburg, Bavaria, Germany

[††]xunlin.qiu@ecust.edu.cn
[‡‡]peng.fang@siat.ac.cn

Received 4 September 2022; Revised 3 December 2022; Accepted 15 February 2023; Published 14 July 2023

Nowadays, the demand for advanced functional materials in transducer technology is growing rapidly. Piezoelectric materials transform mechanical variables (displacement or force) into electrical signals (charge or voltage) and vice versa. They are interesting from both fundamental and application points of view. Ferrooelectrets (also called piezoelectrets) are a relatively young group of piezo-, pyro- and ferroelectric materials. They exhibit ferroic behavior phenomenologically undistinguishable from that of traditional ferroelectrics, although the materials *per se* are essentially non-polar space-charge electrets with artificial macroscopic dipoles (i.e., internally charged cavities). A lot of work has been done on ferroelectrets and their applications up to now. In this paper, we review and discuss mostly the work done at University of Potsdam on the research and development of ferroelectrets. We will, however, also mention important results from other teams, and prospect the challenges and future progress trend of the field of ferroelectret research.

Keywords: Ferroelectret; piezoelectret; space-charge electret; transducer; advanced functional materials.

1. Introduction

Piezoelectric materials transform mechanical variables (displacement or force) into electrical signals (charge or voltage) and vice versa, suitable for a large range of existing or conceivable applications. Some, but not all, piezoelectric materials also exhibit pyroelectricity which transforms temperature variations into electrical currents and are used mainly in sensors, whereas the reverse electrocaloric effect has been more intensively studied only recently.[1] Sometimes, piezoelectricity is also connected with ferroelectricity, which is the existence of a spontaneous and remnant polarization that can be re-oriented in sufficiently high electric fields. Traditional piezoelectric materials include inorganic piezoelectric single crystals and ceramics,[2] piezoelectric polymers[3–5] and piezoelectric ceramic-polymer composites,[6,7] which are all polar materials containing intrinsic dipolar units. In view of this, piezoelectricity is often assumed to be possible only in polar i.e., dipole-containing materials. The family of piezoelectric materials has received a relatively young member, the so-called "ferroelectret" (also called piezoelectret) since about the end of last century.

Ferro- or piezoelectrets are internally charged non-polar polymer foams and polymer-film systems with cavities. Polymer foams are widely used in our daily life, for instance,

[§§]Corresponding authors.

Table 1. Ferroelectric behavior: Evidence in various materials classes (Necessary and sufficient conditions).

Condition for ferroelectric behavior	Single- or multi-crystalline polar material	Semi-crystalline polymer or polymer-based composite	Heterogeneous material with interface charge
Curie Phase Transition	Always Observed	Sometimes Masked	Never Observed
Symmetry Breaking	Induced by Curie Transition (plus Poling)	Induced by Curie Transition plus Poling	Induced by Electric Poling
Spontaneous Polarization	Related to Curie Transition	Related to Curie Transition	So Far Not Observed
Hysteresis Behavior	Dipole Reorientation + Domain Walls	Dipole Reorientation + Crystallite Boundaries	Polarity Switching of Interface Charges

as packaging materials for candies and chocolates.[8] In a ferroelectret, the polymer itself is a space-charge electret that can quasi-permanently capture real charges.[9] The cavities inside the material can be internally charged at high applied electric fields by means of micro-plasma discharges (also known as dielectric barrier discharges or DBDs).[10] Positive and negative charges generated in the DBDs move in opposite directions under the applied fields, and are captured on the internal top and bottom surfaces of the cavities. The charged cavities form macroscopic dipoles whose direction can be switched by reversing the polarity of the applied electric field, showing hysteresis loops phenomenologically undistinguishable from those in traditional ferroelectrics.[11] The materials are named ferroelectrets because their macroscopic dipole polarization exhibits ferroic behavior, while the internal charge trapping is the same as in other space-charge electrets.[12] Table 1 summarizes a few important conditions for ferroelectric behavior in different types of materials.[13] The underlying mechanism of ferroelectrets is quite different from that of typical ferroelectrics. Ferroelectrets contain no intrinsic ionic or molecular dipoles, and hence exhibit no spontaneous polarization and curie phase transition. Their ferroic behavior relies on gas breakdown inside the cavities and subsequent charge trapping on the internal surfaces.

Ferroelectrets not only represent a scientific curiosity, but also possess promising application potential because they combine some of the respective advantages of ferroelectric ceramics (large piezoelectricity) and of polymers (mechanical flexibility and elastic compliance). So far, a lot of studies have been implemented on the fundamentals and applications of ferroelectrets. Also, a number of review articles and book chapters are available. Some survey more general on the field of ferroelectret research.[14–22] Others are more focusing on specific topics of the field, such as on ferroelectret materials,[23] on theoretical models and numerical simulations,[24,25] on measurement techniques,[26–28] on applications in general,[29,30] in health monitoring,[31] in energy harvesting,[32–35] and in air-coupled ultrasonic non-destructive testing.[36,37] In this paper, we review and discuss the state of the art and progress trend in the field of ferroelectret research by covering a broad range of topics, including developments in ferroelectret materials, charging mechanisms and charging methods of high efficiency, fundamental and application-relevant aspects of the piezoelectric activity, and representative applications. We discuss mostly results obtained at University of Potsdam on the research and development of ferroelectrets. We will, however, also mention important results from other teams, and prospect the challenges and future progress trend of the field of ferroelectret research.

2. Ferroelectret Materials

Although it was theoretically predicted already in 1978 that inhomogeneous layer-structured polymer-film systems may exhibit peculiar electret properties,[38] extensive investigation on ferroelectrets was not initiated until around 1990 by Finnish colleagues using cellular polypropylene (PP) foams.[39–41] Then cellular PP has been the workhorse of ferroelectret research for a long time due to a number of advantages such as large piezoelectricity, easy availability and processing, light weight, nontoxicity, low acoustic impedance. However, cellular PP ferroelectrets suffer from two major problems: (1) Inferior thermal stability of the piezoelectricity. The piezoelectric sensitivity decays irreversibly at temperatures above 60°C because of de-trapping of electret charges.[42] (2) A wide and not well-controlled size and shape distribution of the cavity structure. Only a relatively small number of the cavities are optimal for charging and for transducer operation.[43] From a practical point of view, films with well-controlled or even uniform cavity size and shape are very desirable, which allows for large-scale production of the transducer films with good reproducibility. In order to solve one or both of the two problems, much work has been done to introduce new ferroelectrets through a variety of preparation strategies. The development of novel ferroelectrets has been summarized in previous reviews to some extent.[21,23,32]

In general, ferroelectrets that have been developed so far can be classified into the following three categories.

2.1. *Ferroelectrets with cellular structure*

Cellular PP ferroelectrets belong to this category. The know-how acquired from the research and development of cellular PP ferroelectrets is employed to develop cellular film ferroelectrets from other polymers. The first example is porous amorphous fluoropolymer (Teflon-AF) ferroelectret reported by Mellinger *et al*.[44] Teflon AF dissolves easily in a perfluorocarbon solvent, which is a big advantage as compared with other fluoropolymers such as polytetrafluoroethylene (PTFE). Boiling the solvent during drop-casting produces porous Teflon-AF films of 3–10 μm thickness. Several layers were drop cast on top of each other in order to get the desired thickness, and then the open pores were sealed at 180°C with solid Teflon AF films drop-casted at room temperature. After corona charing and electrode metalization, the porous Teflon-AF ferroelectrets show piezoelectric d_{33} coefficients of up to 600 pC/N at temperatures of at least 120°C. The Teflon-AF ferroelectrets have much better thermal stability than cellular PP ferroelectrets.

Wegener *et al*. studied the suitability for ferroelectrets of cellular poly(ethylene terephthalate) (PETP) foams from an industrial production line.[45] It was found that the as-received PETP foams (with thicknesses of 160 ± 10 μm and densities between 0.37 and 0.40 g/cm^3) are over-inflated and do not show detectable piezoelectric sensitivity even after being charged with very high electric fields. By annealing the PETP foams at temperatures between 70 and 160°C, the film thickness can be reduced, while the cellular foam structures do not collapse. An annealed cellular PETP film with a density of 0.67 g/cm^3 and an elastic modulus of about 7 MPa reaches a maximum piezoelectric d_{33} coefficient of 23 pC/N. The piezoelectric sensitivity is thermally stable up to 65°C, slightly better than that of cellular PP ferroelectrets.

The PETP ferroelectrets made of commercially available foams are still rather stiff and show relatively small piezoelectric sensitivity. Wirges *et al*. proposed a new method for preparing cellular PETP ferroelectrets from commercial non-voided PETP films.[46,47] This method consists of an optimized sequence of processing steps including foaming, biaxial stretching (sometimes with gas-diffusion expansion after stretching), and electric charging. First, solid PETP films are foamed through physical foaming with supercritical carbon dioxide (scCO$_2$). It is well known that supercritical CO$_2$ penetrates relatively easily into several polymers and plasticizes them.[48,49] Carbon dioxide turns into a supercritical state at pressures higher than 73 bar and temperatures exceeding 31°C.[50] For foaming, non-voided PETP films are stored in a chamber filled with high-pressure scCO$_2$ for sufficiently long period of time, allowing the scCO$_2$ to penetrate into the films and eventually saturate. Then, the pressure in the chamber is quickly released within several seconds, and the films filled with scCO$_2$ are thermally treated at a suitable elevated temperature. The PETP films are foamed due to a sudden phase change of the scCO$_2$ into gas. Compared with chemical foaming with a blowing agent, the physical foaming using scCO$_2$ does not cause any pollution or impurities. Treatment with scCO$_2$ at 100 bar for up to 9 h and heat treatment at temperatures between 110 and 210°C for 10 s can foam the PETP within a density range from 1.36 to 0.33 g/cm^3. Then, the foamed structures may be further optimized by means of well-controlled biaxial stretching and inflation through gas-diffusion expansion.[51–54] The SEM image of Fig. 1(a) shows the structure of a cellular PETP film that is foamed, stretched and inflated. Finally, the PETP foams are corona charged with a point voltage of up to 60 kV in 3 bar SF_6 atmosphere. The optimized PETP foam shows a low elastic modulus of 0.3 MPa and a high piezoelectric d_{33} coefficient of 476 pC/N.

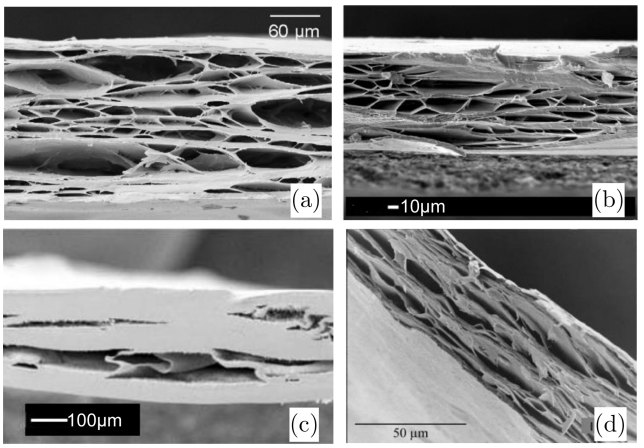

Fig. 1. Cross-sectional scanning-electron-microscope (SEM) images of (a) A cellular PETP film foamed by scCO$_2$ treatment at 100 bar for 9 h, heat treatment at 190°C for 10 s, optimized by biaxial stretching with a ratio of 150% at 230°C, and then inflation by gas-diffusion expansion with 25 bar nitrogen.[47] (b) A cellular PENP film that is prepared by foaming (scCO$_2$ at 150 bar for 5 h, and a heat treatment at 130°C for 10 s), inflation (150 bar scCO$_2$ treatment for 19 h plus a heat treatment at 130°C for 10 s), and biaxially stretching (at a ratio of 1.5).[56] (c) An FEP foam 272 μm in thickness and 1.57 g/cm^3 in density on average. Foaming conditions: scCO$_2$ treatment at 150 bar for 16 h at RT, and then at 200 bar for 2 h at 75°C in a high-pressure steel chamber. The pressure in the chamber was reduced to normal atmospheric pressure, and the FEP film was taken out and subjected to a heat treatment at 200°C for a few seconds.[59] (d) A COP foam prepared by biaxially stretching a COP cast film containing suitable inorganic filler particles.[61]

Poly(ethylene naphthalate) (PENP) is another thermplastic polyester with molecular structure similar to that of PETP. The only difference is the stiffer double aromatic ring of naphthalate group instead of the single one of terephthalate present in PETP. Due to the double ring structure, PENP has improved thermal, mechanical, electrical and barrier properties, as well as chemical, hydrolytic and radiation resistance as compared with PETP. Particularly, PENP has much better

charge stability than PETP.[55] Fang *et al*. prepared cellular PENP ferroelectrets from commercial solid films through foaming and inflation in $scCO_2$, biaxial stretching, electrical charging, and metallization, namely, processing steps similar with those for PETP ferroelectrets.[56–58] The solid PENP films are foamed by storing in $scCO_2$ with a pressure between 100 to 200 bar for several hours and then a heat treatment at elevated temperatures. To further optimise the cellular structure, the PENP foams are subjected to inflation and biaxially stretching. Figure 1(b) shows the cross section of a cellular PENP film. The foamed PENP films are corona charged for 15 s either in normal air with a point voltage of 21 kV or in 3 bar SF_6 with 50 kV. Piezoelectric d_{33} coefficients up to 140 pC/N are obtained for samples with a density of about 1.0 g/cm^3, and the piezoelectricity is stable at least up to 80°C. Even at 100°C, the cellular PENP ferroelectrets are still piezoelectically active.

Fluorinated ethylene propylene (FEP), a copolymer of tetrafluoroethylene (TFE) and hexafluoropropylene (HFP), is known to possess excellent charge stability for both polarities after charging at elevated temperatures.[9] Voronina *et al*. fabricated cellular FEP films by foaming with $scCO_2$ and a subsequent controlled inflation with heat treatment, similar with the above-mentioned processing steps for cellular polyester ferroelectrets.[59] The obtained cellular FEP films usually contain one or two large voids across the film thickness (Fig. 1(c)). After corona charging in 3 bar SF_6 with 60 kV. The cellular FEP ferroelectrets show piezoelectric d_{33} coefficients up to 50 pC/N. Due to the quite large cavities, the cellular FEP films have uneven surface, and the piezoelectric sensitivity strongly decreases with increasing static pressure. The d_{33} coefficient becomes negligibly small at static pressures larger than about 60 kPa.

Cyclo-olefin-based polymers are nonpolar space-charge electrets with excellent charge stability for both positive and negative polarity[60] and therefore are promising base materials for ferroelectrets of high service temperature. Traditionally, polymer foams are fabricated by using chemical or physical foaming agents in molten polymer.[40] One method widely used in industry is stretching filler-loaded polymers under suitable conditions. Fillers such as mineral particles are added to the polymer melt before it is biaxially stretched. The fillers serve as stress concentrators around which microcracks are created during stretching of the film. Using this method, Wegener *et al*. and Saarimäki *et al*. prepared foams from cyclo-olefin polymers and copolymers.[61,62] For sample preparation, cyclo-olefin polymers were blended with lower-T_g olefin polymers in order to improve the elastic properties (and thus the processability). The trade-off between low elastic stiffness and high thermal stability should be carefully considered. Five wt.% mineral particles with an average diameter of 2 μm were added to and properly mixed with the polymer compounds before film casting. To form cellular structure, the cast COC and COP films were biaxially drawn at suitable temperature with a draw ratio between 3 and 5.

The obtained cellular structure can be further optimized through a gas-diffusion expansion procedure combined with thermal treatment. Figure 1(d) shows the cross-sectional SEM of a cellular COP film. Charging of the samples was done either by corona charging in SF_6 with a point voltage of up to 60 kV or by direct contact charing in air with an electrode voltage of about 4 kV. The charged cellular cyclo-olefin ferroelectrets typically exhibit piezoelectric d_{33} coefficients of about 15 pC/N. The d_{33} coefficient is more than one order of magnitude smaller than that of cellular PP ferroelectrets. Nevertheless, the piezoelectric sensitivity of some of the new cyclo-olefin ferroelectrets is thermally stable at temperatures up to 110°C, markedly better than that of cellular PP and PENP ferroelectrets.

Still another type of polymer films with foamed strucutre are open-porous PTFE films that are usually made by uniaxially strechting PTFE rods by means of two pairs of cylinders with different speeds. The rods are fabricated through extrusion of commercial resin at high temperature. It was reported that porous PTFE shows excellent surface-charge storage stability at temperatures up to 300°C, due probably to the much larger surface area and more local defects that can serve as traps.[63] With a thermal treatment composed of heating at 320°C for 2 min followed by sudden quenching in liquid nitrogen, the charge stability of porous PTFE can be further improved.[64] The charging behavior and piezoelectric properties of porous PTFE films have been investigated in several works.[65–72] Porous PTFE films with press-on electrodes show large piezoelectric d_{33} coefficients of up to several hundred pC/N. However, the d_{33} is drastically deteriorated by metalization of electrodes. During metalization, the metallic particles go into the interfaces between the cavities and the dielectric because of the open-porous structure. Consequently, the interface charges are lost and the piezoelectricity of the film becomes extremely low.

2.2. *Ferroelectrets with soft/hard multi-layer structure*

Inhomogeneous layer-structured film systems with space charge trapped on the interfaces were already employed in early studies of the piezoelectric response of space-charge electret systems.[73,74] For this type of ferroelectrets, the elasticity difference among the soft/hard layers and the density of the interface charge is the most critical parameter for the piezoelectric sensitivity of the samples. Figure 2(a) schematically shows the cross-section of a bi-layer ferroelectret consisting of a soft and a hard electret film. Porous PTFE films are particularly suitable for the soft layers because of their high softness and extremely low conductivity. Gerhard-(Multhaupt) *et al*. investigated multi-layer stacks consisting of at least one "hard" non-porous and at least one "soft" porous PTFE film as ferroelectrets.[71,72,75,76] Individual films were corona charged before assembly. It was found that the piezoelectric sensitivity of the stacks increases linearly with the density of the interface charge and strongly depends on

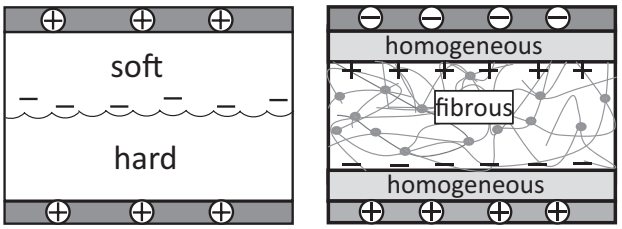

Fig. 2. Schematic cross-section of ferroelectrets with soft/hard multilayer structures. (a) A heterogeneous ferroelectret consisting of elastically "soft" and "hard" electret films. The bi-layer structure is charged at the interface between the two electrets. Piezoelectricity originates from the asymmetrical displacement of interface charges relative to the electrodes under mechanical stress. (b) A three-layer ferroelectret composed of two homogeneous electret (hard) films and a highly porous (soft) layer in between. The sample can be charged by means of dielectric barrier discharges in sufficiently high electric fields. Charges of both polarities are generated and eventually captured on the internal surfaces of the homogeneous electret layers, thus forming macroscopic dipoles.

the geometry of the stacks. In general, the highest piezoelectric d_{33} coefficients of the stacks are comparable with the respective coefficients of the best ferroelectric polymers.

Non-porous PTFE has outstanding electret properties and thermal stability, but on the other hand it cannot be easily processed with typical thermal and solution methods. By using other non-porous polymers with better processability than PTFE, it is possible to have tight bonding between the non-porous polymer layer(s) and the porous PTFE layer via techniques such as thermal bonding and spin-coating, such that one or both surfaces of the porous PTFE are sealed with the non-porous layers. Such multi-layer film systems have mechanically stable structure. More importantly, the outer non-porous surfaces of the samples can be metallized, without destroying the interfacial charge. Wegner *et al*. prepared porous PTFE coated with non-porous polymers including polystyrene (PS), PETP and Teflon AF.[77,78] Porous PTFE with coating on one surface exhibits higher surface potentials than the non-coated PTFE. The PTFE/Teflon AF layer systems show a piezoelctric d_{33} coefficient of 5 pC/N. Schwödiauer *et al*. prepared hybrid fluoropolymer systems consisting of a porous PTFE and a perfluorinated cyclobutene (PFCB) layer.[79] The latter is an amorphous crosslinked, low permittivity fluoropolymer with excellent charge stability comparable with PTFE.[80] The porous PTFE/PFCB double layer systems charged at the interface yield a large quasi-static piezoelectric d_{33} coefficient of 600 pC/N.

Figure 2(b) schematically shows another type of layer-structured ferroelectrets. In such ferroelectrets, homogeneous electret films (hard layers) are separated by highly porous layers (soft layers) in between. The high porosity of the soft layers allows for charging of the sample with dielectric barrier discharges in a sufficiently high applied electric field. Charges of both polarities are generated and eventually captured on the internal surfaces of the homogeneous electret layers, thus forming macroscopic dipoles. Von Seggern *et al*. prepared ferroelectrets by sandwiching a highly porous PTFE, so-called expanded PTFE (ePTFE) consisting of up to 98% air, between two solid FEP layers.[81–84] By removing the air gaps at the surface of the ePTFE via evacuation, the contact between the FEP and the ePTFE films was strengthened. Due to the extremely high softness of the ePTFE, the sandwiches show very high quasistatic piezoelectric d_{33} coefficient. However, the samples are not very stable, and the d_{33} coefficient decays from 800 to 400 pC/N in six days after charging.[81] A strong decrease in the d_{33} coefficient with increasing frequency and static pressure is also observed. In the study of Zhang *et al*., laminated PTFE films consisting of porous PTFE films and nonporous FEP[85] or PTFE[86,87] films were prepared by thermal bonding or sintering under high pressure, respectively. In this way, the open pores of the porous PTFE films are closed by the nonporous FEP or PTFE films with strong bonding, which renders the samples mechanically stable. The samples typically show high quasi-static piezoelectric d_{33} coefficients of more than several hundred pC/N, and remain piezoelectrically active at temperatures of up to 120°C.

2.3. *Ferroelectrets with regular cavity structure*

Both types of the above-mentioned ferroelectrets, namely, ferroelectrets with cellular structure and ferroelectrets with soft/hard multi-layer structure, have a relatively wide and not well-controlled size and shape distribution of the cavities. Much effort has been devoted to developing ferroelectrets with regular cavity structure. Altafim *et al.* prepared bi-layer FEP ferroelectrets with regular millimeter-scale cavities via a vacuum-assisted thermal fusion.[88] Stacks of two FEP films were put on a metal grid connected to a vacuum pump. By evacuation from one side of the metal grid, the adjacent FEP film on the other side was sucked into the regular openings of the grid. Heating and pressing a metal plate onto the stack at suitable temperatures result in film systems with air cavities of the same diameter as the grid openings. After internal charging by means of high impulse voltages, the bi-layer FEP ferroelectrets show quasi-static d_{33} coefficients of up to 500 pC/N, which strongly decrease with increasing applied pressure. Basso *et al*. fabricated three-layer ferroelectrets with regular cavities by thermal fusion of sandwiches consisting of two homogeneous FEP films and a PTFE film with regular holes in between.[89] Regular holes with millimeter and tens of μm diameters were made by mechanical drilling and laser perforation, respectively. After charging, the three-layer ferroelectrets show a piezoelectric d_{33} coefficient of about 10 pC/N, confirming the feasibility of the proposed method for ferroelectrets with regular cavity structures.

Later, Altafim *et al*. proposed a straightforward lamination process for making ferroelectrets with well-controlled and uniform cavities.[90,91] In this process, sandwiches of two

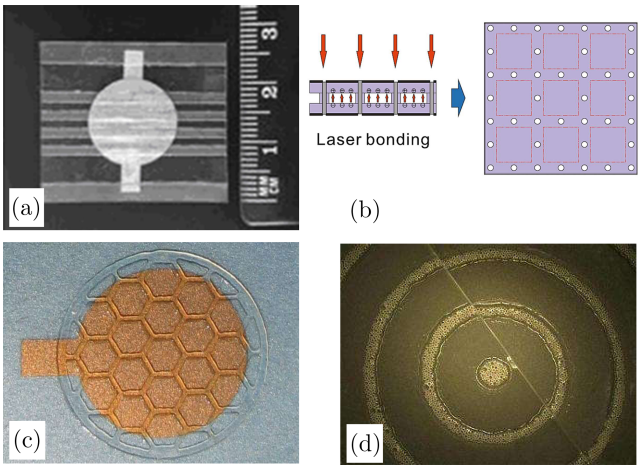

Fig. 3. Ferroelectrets with regular cavity structure. (a) Tubular-channel FEP ferroelctrets made by thermal lamination.[90] (b) Three-layer FEP ferroelectrets prepared by laser cutting, laser bonding, electrode evaporation, and high-field poling.[99] (c) A polymer-ferroelectret system consisting of two uniform polycarbonate films and an adhesive-tape template in between. The outer surface of the PC films were metallized with semitransparent gold electrodes 20 nm in thickness.[100] (d) A screen-printed three-layer polymer system for ferroelectret.[102]

electret films and a template with pre-designed pattern of openings are thermally laminated at suitable temperatures. The electret films are fused with each other through the openings of the template. Afterwards, the template is removed, resulting in a polymer-film system with regular cavities of the designed pattern. Sandwiches of two homogeneous FEP films and a PTFE template in between were laminated at 300°C. The PTFE template contained several evenly distributed parallel rectangular openings. FEP film systems with tubular-channel cavities were obtained by cutting and taking out the PTFE template after lamination. Figure 3(a) shows a photo of a tubular-channel FEP ferroelectret with aluminum electrodes on both surfaces. Such FEP ferroelectrets exhibit high piezoelectric d_{33} coefficients of up to 160 pC/N, which is stable at temperatures of at least 130°C. The regular open channel design offers also other advantages through the layered lamination approach. In Ref. 92, Altafim *et al*. showed that adding layers on top of the ferroelectret channels can bring new functionalities. The addition of the magnetic stripes rendered the ferroelectret sensors magnetically sensitive, resulting in piezoelectric-magnetic response of more than 150 pC/T.

Fluoropolymer stack ferroelectrets have also been developed by combining molding (for introducing the desired cavity patterns) and thermal fusion (for bonding the adjacent layers). In general, there are two kinds of production strategies. In one strategy, molding of the pre-designed patterns is implemented during thermal fusion.[93,94] A metal mesh with (sub) millimeter spacing was pressed onto PTFE and FEP film stacks, which, in combination with a thermal treatment at 280°C (higher than the melting point of 260°C of FEP), leads to thermal fusion of the polymer layers underneath the wires of the mesh and formation of regular cavities between the fused areas. In another strategy, molding of FEP or PTFE films is implemented prior to thermal fusion of film stacks either by cold pressing at room temperature[95–97] or hot pressing at certain elevated temperatures.[98] Rigid template(s) with pre-designed patterns, often together with soft rubber pad(s), are employed for the molding. Then, the patterned polymer films are stacked, sometimes with non-patterned homogeneous films in between, and thermally fused at temperatures slightly higher than the melting point of FEP. After charging and electrode evaporation, such fluoropolymer ferroelectrets often show quasi-static piezoelectric d_{33} coefficients of hundreds to one thousand pC/N, which is thermally stable up to 120°C.

FEP film sandwiches of two homogeneous outer layers and a middle layer with regular openings can also be bonded locally by means of a laser beam.[99] As schematically shown in Fig. 3(b), an FEP mesh with square openings prepared by laser cutting was sandwiched between two FEP films with their outer surfaces metallized. The sandwiches were locally bonded by means of a laser beam at selected positions (white circles in the right-hand part of Fig. 3(b)), thus forming three-layer film systems with regular cavities. Internal poling of the cavities was implemented prior to the laser bonding. The piezoelectric properties of the samples were studied by means of dielectric resonance spectra[26] and acoustical measurements.[27] Piezoelectric d_{33} coefficients of a few hundred pC/N are achieved. The piezoelectric sensitivity shows a relatively flat frequency response in the range between 300 Hz and 20 kHz, and is thermally stable up to at least 120°C.

Besides fusion bonding, electret film layers may also be bonded through a sticky material. Qiu *et al*. reported polycarbonate ferroelectrets composed of two PC films bonded with a sticky template made of a double-sided adhesive tape.[100] The adhesive-tape template with honeycomb-shaped openings was made by computer-controlled laser cutting. The side length of the hexagonal openings is 1.5 mm, and the width of the remaining adhesive tape ridges is 0.5 mm. PC films were metallized on one surface with aluminum or gold electrodes. By sandwiching the adhesive-tape template with two PC films via their nonmetallized surfaces, a three-layer film system with well-defined cavities was obtained. Figure 3(c) shows a photo of a three-layer film system with 20 nm thick semitransparent gold electrodes. The structure of the adhesive-tape template is clearly visible. After contact charging with a voltage of 2 kV, the three-layer PC ferroelectrets show piezoelectric d_{33} coefficients of about 30 pC/N. Rychkov *et al*. prepared unipolar ferroelectrets by gluing corrugated FEP films to aluminum foils.[101] The corrugated FEP films were created by the same lamination process as in Ref. 90 with the exception that two-layer stacks of only one FEP film and one PTFE template were laminated. The unipolar FEP ferroelectrets, with essentially the same geometry

as an electret microphone, show d_{33} coefficients of about 45 pC/N.

In another study, Sborikas *et al*. developed three-layer PC ferroelectrets by means of screen printing.[102] Screen printing is widely employed for two-dimensional patterning of printed layers. For sample preparation, an ink formulation consisting of 97.6% monomer (Desmolux u680H) and 2.4% photo-initiator (Darocure 1173) was screen-printed onto a polycarbonate film with pre-designed patterns (ring structure in the present case). Then another PC layer was placed on the printed ink layer. After annealing at 110°C for 4 h, the PC films were tightly bonded to each other by the ink pattern, yielding a film system with well-defined cavities. A photo of one sample is displayed in Fig. 3(d)). Silver-paste electrodes were screen-printed onto both outer surfaces of the samples, and direct contact charging was carried out with a voltage of up to 6 kV. Typical piezoelectric d_{33} coefficients of about 30 pC/N are obtained for the screen-printed PC ferroelectrets, which possess thermal stability up to 100°C.

More recently, three-dimensional (3D) printing technique has been employed in producing ferroelectrets with regular cavity structures. First examples of this kind are 3D-printed acrylonitrile butadiene styrene (ABS) ferroelectrets with well-defined cavities, which show piezoelectric d_{33} coefficients of up to 100 pC/N and thermal stability up to 85°C.[103,104] Assagra *et al*. reported 3D-printed PP ferroelectrets with regular chess-pattern cavities of precisely controlled size and shape using standard 3D-printing parameters.[105,106] After charging, the samples exhibit piezoelectric coefficients up to 200 pC/N. The piezoelectric sensitivity of 3D-printed PP ferroelectrets and its temporal and thermal stability are similar with those of cellular PP ferroelectrets. These interesting works demonstrate the feasibility of 3D printing techniques for developing novel ferroelectrets.

Ferroelectrets with regular cavity structures have also been developed by several other techniques. Li and Zeng reported a $scCO_2$-assisted assembling method.[107] In $scCO_2$, the surface glass transition temperature of COC becomes substantially lower than that of the bulk due to strong COC-CO_2 interaction. Therefore, COC film stacks consisting of homogeneous films and films with regular openings can be tighly bonded at a temperature much lower than the melt ing point. The obtained COC ferroelectets show d_{33} coefficients of up to 1000 pC/N with a thermal stability of up to 110°C. Wang *et al*. prepared ferroelectrets using microfabrication technique.[108,109] Multi-layer PDMS films with regular cavities were prepared by a sequence of casting and stacking steps using a photoresist mold placed on a silicon wafer. The internal surfaces of the cavities were coated with a thin layer of Teflon AF by filling and then drying a solution of Teflon AF. After DBD charging, negative and positive charges are deposited onto the top and bottom internal surfaces of the Teflon AF layers, respectively. Thus, in the microfabricated ferroelectrets, the Teflon AF layers offer excellent charge storage, and the PDMS structures supply large deformation of the macroscopic dipoles (internally charged cavities). Such samples show d_{33} coefficients of more than 1000 pC/N.

3. Charging of Ferroelectrets

As in the case of ferroelectric polymers such as β-PVDF, charging/poling is a critical procedure for the preparation of ferroelectrets. However, the mechanism of charging is quite different between ferroelectrics and ferroelectrets. For ferroelectric polymers, poling is carried out to align molecular dipoles into the direction of the applied electric field. Ferroelectrets are space-charge electrets without molecular dipoles. Except for soft/hard layer-structured systems with interfacial charges where the related surfaces are charged by e.g., corona charging prior to the assembling, ferroelectrets with cavities are internally charged by a series of dielectric barrier discharges (DBDs) in sufficiently high electric fields.

3.1. *Charging mechanism of ferroelectrets*

Charging of ferroelectrets is accomplished by a series of dielectric barrier discharges (DBDs).[110] In DBDs, at least one side of the discharge gap is insulated from the electrodes by a dielectric layer.[10] Figure 4 schematically shows the charging process of a ferroelectret with cellular structure. DBDs are triggered by applying electric fields higher than the threshold for breakdown in the cavities. DBDs are micro-plasma discharges which generate positive and negative charges of the same amount. Under the applied electric field, the charges of opposite polarity move in opposite directions and are eventually trapped at internal top and bottom surfaces of the cavities. Internally charged cavities can be regarded as man-made macroscopic dipoles, in analog to molecular dipoles in ferroelectrics.

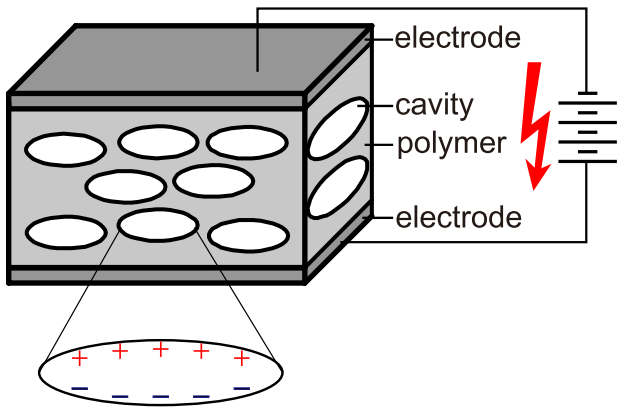

Fig. 4. Schematic charging process of ferroelectrets. Dielectric barrier discharges are triggered in the cavities by applying a sufficiently high electric field, generating charges of both polarities. Positive and negative charges travel in opposite directions under the applied electric field and are eventually trapped on the internal surfaces of the cavities.

The triggering of DBDs in ferroelectrets is controlled by Paschen's law which, according to Townsend's model, states that the breakdown voltage between parallel plates in a gas is a function of pressure p and electrode spacing d (equal to the cavity height in context of ferroelectret),

$$V_{th} = \frac{Apd}{B + \ln(pd)}, \tag{1}$$

where B is given by

$$B = \ln\left(\frac{C}{\ln(1+1/\gamma)}\right). \tag{2}$$

A and C are gas-dependent constants. For air, A and C of 273.8 $Vm^{-1}Pa^{-1}$ and 11 $m^{-1}Pa^{-1}$ are experimentally defined, respectively, and γ of 0.01 is the so-called second ionization coefficient. Mellinger *et al*. suggested that A and C might need to be adjusted for micrometer-sized cavities.[111]

According to the above discussion, a threshold behavior with respect to the charging voltage can be expected for the charging and the resulting piezoelectric sensitivity of ferroelectrets (similar to the "coercive" phenomenon of ferroelectrics). Wegener *et al*. studied the threshold behavior of cellular PP ferroelectrets by means of corona[112] and direct contact charging.[113] They observed that the d_{33} coefficients of the samples are almost zero below the threshold charging voltages, and increase drastically with increasing charging voltage above the respective threshold. Based on a simplified model for ferroelectrets,[114,115] Zhang *et al*. theoretically studied the charging process in cellular PP ferroelectrets.[116] The analysis focuses on the local electric fields of the cavities, which is the sum of the applied charging field E_{app} and the field induced by the internally trapped charges E_{ind}. When a fresh sample is charged with increasing voltage, the effective polarization P_{eff}, i.e., the density of the macroscopic dipoles, is zero below the threshold voltage V_{th} (corresponding to the breakdown field E_{th}). Above V_{th}, DBDs take place in the cavities, depositing charges onto the internal top and bottom surfaces. The trapped charges induce an electric field opposite to the applied one, and therefore partly compensate the external field. DBDs extinguish as long as the local electric field becomes lower than the V_{th} again. With increasing charging voltage V_{app}, DBDs keep occurring and P_{eff} increases linearly with V_{app}. Therefore, when a fresh sample is charged with increasing voltage, the effective polarization at the respective V_{app} is given by[116]

$$P_{eff} = \begin{cases} 0 & (V_{app} < V_{th}), \\ k(V_{app} - V_{th}) & (V_{app} \geq V_{th}), \end{cases} \tag{3}$$

where k is a sample-specific parameter. When the charging voltage is switched off, only E_{ind} is present. Similarly, if E_{ind} is higher than E_{th} (which happens when V_{app} is higher than $2V_{th}$), DBDs will be triggered in the opposite direction (so-called back discharges). In this case, P_{eff} will be reduced until the local field is equal to E_{th}. The effective remnant polarization (the polarization after the voltage has been turned off) can be expressed as

$$P_{rem} = \begin{cases} 0 & (V < V_{th}), \\ k(V - V_{th}) & (V_{th} \leq V \leq 2V_{th}), \\ kV_{th} & (V > 2V_{th}). \end{cases} \tag{4}$$

From Eq. (4), P_{rem} of ferroelectrets is zero below the threshold charging voltage. P_{rem} then increases linearly with V_{app} and saturates at charging voltages higher than $2V_{th}$. Zhukov and von Seggern suggested a similar analysis for layered fluoropolymer ferroelectrets (FEP-ePTFE-FEP sandwiches).[117]

DBDs in ferroelectrets always emit light signals that can be easily detected as a diagnostic tool for characterizing the charging process. The light emission stems from electronically excited and/or ionized gas molecules inside the cavities. In early studies, light emission from the DBDs in cellular PP ferroelectrets was photographed by means of digital cameras.[110,112] Qiu *et al*. studied the light emission using highly sensitive photomultiplier (PMT) and PC-controlled electron-multiplying charge-coupled device (EMCCD) camera.[58,97,118–122] The sample, metallized on both surfaces with 20 nm thick semi-transparent gold electrodes, was mounted in a light-tight chamber for synchronous light detection from both sides. Figure 5 shows spatially-resolved EMCCD photographs of a cellular PP ferroelectret under a charging voltage that ramps up linearly from 0 to 6 kV within 1 s.[118] Detectable light emission occurs at t = 0.5 s, corresponding to a threshold charging voltage of 3 kV. In general, the light emission is seen as a diffuse glow due to strong light scattering of the cellular structure. DBDs in

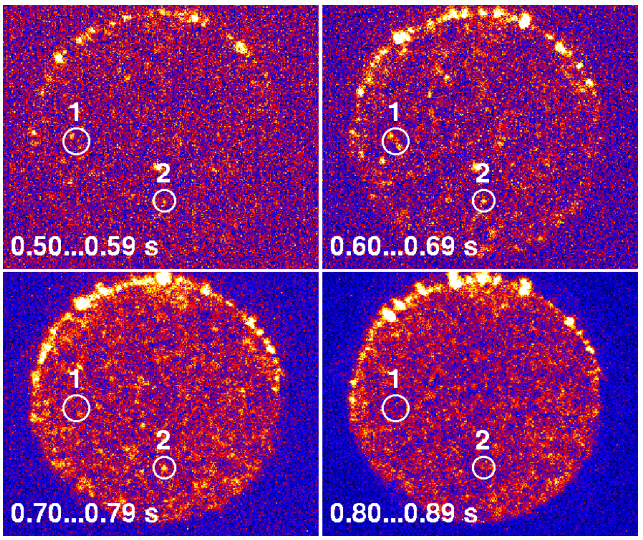

Fig. 5. False-color EMCCD images of a cellular PP ferroelectret. The charging voltage was ramped up to 6 kV in 1 s, starting at 0 s. Each frame was exposed for 90 ms. Circles 1 and 2 show light emission from some of the large cavities. The strong light emission at the upper periphery is caused by corona discharge at the electrode edge.[118]

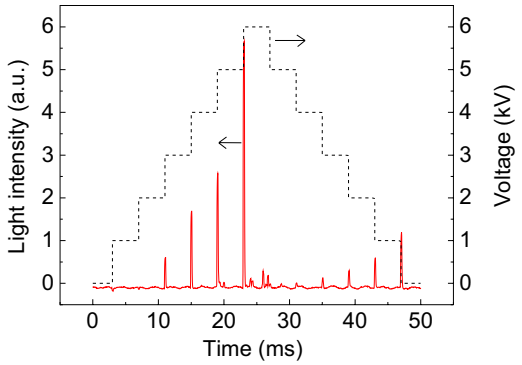

Fig. 6. Light emission of a cellular PP ferroelectret as a function of time measured by means of a photomultiplier (left ordinate). The charging voltage is increased and then decreased in steps of 1 kV (right ordinate).[119]

some of the large cavities near the surface are clearly visible (marked with circles 1 and 2) in a specific voltage range.

The light emission can also be quantitatively measured by means of a PMT. In this case, the surface of the sample facing the PMT was covered by masks with a circular hole 8.5 mm in diameter (smaller than the electrode diameter of 16 mm) in order to block light from the corona discharge at the electrode edge. Figure 6 shows the light emission of the cellular PP ferroelectret sample under a stepwise increasing and then decreasing voltage waveform.[119] Again, light emission is observed when the voltage reaches 3 kV, consistent with the EMCCD results. The light intensity strongly increases when the voltage increases further because DBDs are triggered in more and more cavities. Due to the choke effect of DBDs,[10] the light emission takes place at the beginning of each relevant voltage step and then extinguishes very fast to the noise level of the PMT. As can be seen from Fig. 6, light emission appears again when the voltage decreases from 6 kV back to about 3 kV, which is attributed to the above-mentioned back discharges.

The optical emission spectrum (OES) contains important information for characterizing DBDs. The OES of the light emission of cellular PP ferroelectrets was recorded by means of a spectroscopic system consisting of an optical fiber, a monochromator, and the EMCCD camera. The spectrum indicates that DBDs in ferroelectrets originate from the second positive system (SPS) of molecular nitrogen and the first negative system (FNS) of N_2^+, as typically observed with DBDs in air.[119] Particularly, occurrence of the FNS of N_2^+ indicates the ionization of molecular nitrogen, a direct proof of charge generation in the charging process of ferroelectrets. Based on a spectroscopic analysis of the band strength ratios, the electric field during charging of the cellular PP ferroelectret is determined to be in the range between 21 and 28 MV/m, in good agreement with the Townsend breakdown model. Therefore, investigation of the light emission may provide important information for better understanding and further optimization of the charging process of ferroelectrets.

A polarization-*versus*-electric-field (*P-E*) hysteresis is a typical feature for ferroelectric materials. From the hysteresis curves, important parameters such as coercive field and remanent polarization can be determined. Qiu *et al*. investigated the hysteresis behavior of ferroelectrets by means of an *in-situ* acoustical measurements in combination with dielectric resonance spectroscopy.[123] Based on the simplified model consisting of alternating parallel polymer and gas layers,[114,115] the thickness change Δs of a ferroelectret under an external voltage can be expressed as

$$\Delta s = \frac{s}{Y}\frac{\varepsilon_p s_1 \sigma_{eff} V - \frac{1}{2}\varepsilon_0 \varepsilon_p^2 V^2}{(s_1 + \varepsilon_p s_2)^2}, \tag{5}$$

where V is the applied external voltage, Y is Young's modulus of the sample, ε_0 and ε_p are the permittivity of free space and the relative permittivity of the polymer, respectively. s_1 and s_2 are the total thickness of the polymer and the gas layers, respectively, and the total film thickness $s = s_1 + s_2$. σ_{eff} is the so-called effective polarization of ferroelectrets, which equals $\Sigma s_{2i}\sigma_i/\Sigma s_{2i}$, where s_{2i} and σ_i are the thickness of the i^{th} gas layer and the charge density on the surface of the i^{th} polymer layer. Equation (5) indicates that the development of σ_{eff} and V can be monitored by measuring the vibration of the sample (Δs). The idea is to apply a voltage $V = V_{dc} + V_0 \sin(\omega t)$ containing both a dc and an ac component. The dc component is the charging voltage, while the ac part generates measurable acoustic signal. From Eq. (5), one gets

$$\Delta s = \frac{s}{Y(s_1 + \varepsilon_p s_2)^2}\left\{-\frac{1}{2}\varepsilon_0 \varepsilon_p^2\left(V_{dc}^2 + \frac{1}{2}V_0^2\right) + \varepsilon_p s_1 \sigma_{eff} V_{dc} + [\varepsilon_p s_1 \sigma_{eff} - \varepsilon_0 \varepsilon_p^2 V_{dc}]V_0 \sin(\omega t) + \frac{1}{4}\varepsilon_0 \varepsilon_p^2 V_0^2 \cos(2\omega t)\right\}, \tag{6}$$

where the first and the second terms denote bias thickness change independent of the frequency of the ac voltage, the third term arises from the piezoelectric effect, and the last term is the second harmonic term from the Maxwell stress. The third term in Eq. (6) indicates that both the effective polarization and the dc voltage contribute to the radiated sound signal at the fundamental frequency. The effective piezoelectric coefficient at V_{dc} is expressed by

$$d_{33} = \frac{s}{Y}\frac{\varepsilon_p s_1 \sigma_{eff} - \varepsilon_0 \varepsilon_p^2 V_{dc}}{(s_1 + \varepsilon_p s_2)^2}. \tag{7}$$

Figure 7(a) shows the acoustic signal at 1 kHz as a function of the dc voltage. A fresh sample was measured in an anechoic chamber by means of a microphone. In total, three half cycles of the dc voltage were applied, namely, a positive half cycle followed by a negative and a second positive half cycle. At the beginning, the acoustic signal increases linearly with V_{dc}, since σ_{eff} is zero. However, when V_{dc} exceeds the threshold of about

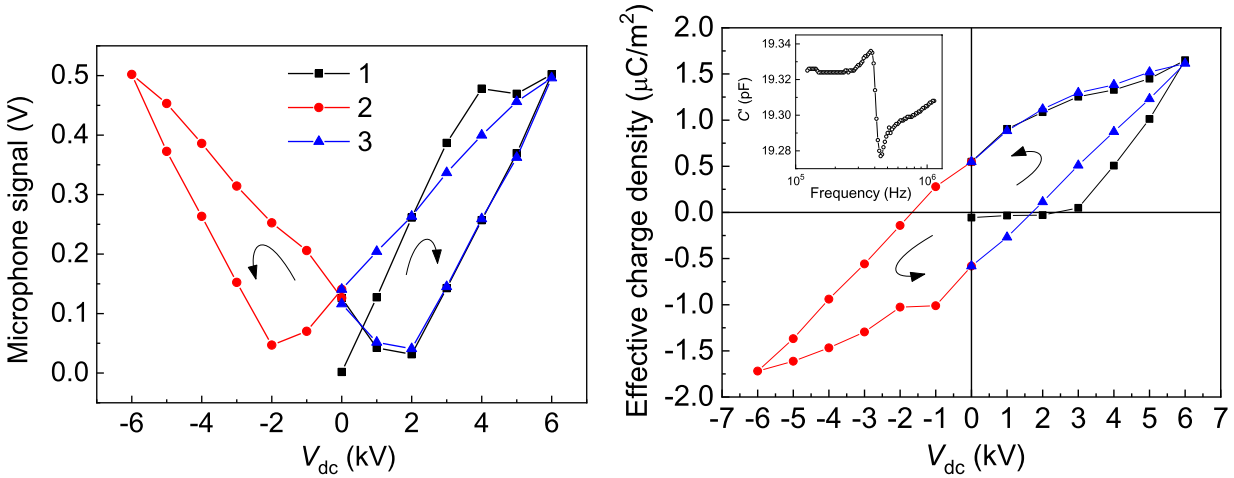

Fig. 7. (a) Butterfly curves of a cellular PP ferroelectret measured by means of an *in-situ* acoustical method on a fresh, uncharged sample with a thickness of 72 μm. Measurements were run with a positive half cycle (curve 1), followed by a negative half cycle (curve 2) and subsequently a second positive half cycle (curve 3). (b) Effective charge density σ_{eff} (calculated from the experimental data shown in (a) as a function of V_{dc}). Inset: The dielectric resonance spectrum for determination of the absolute d_{33} coefficient corresponding to the zero-field microphone signal. Arrows denote the progress of the measurements.[123]

3 kV, the slope of acoustic signal *versus* V_{dc} starts to decrease, since DBDs are triggered in the cavities, introducing nonzero σ_{eff}. According to Eq. (7), V_{dc} counteracts with the induced σ_{eff} regarding the contribution to the acoustic signal. Consequently, when V_{dc} is ramped down from its maximum, the acoustic signal is noticeably lower than the corresponding value during ramping up. The acoustic signal reaches a minimum, then increases again as V_{dc} decreases further and passes through zero, forming a characteristic "butterfly" curve. Butterfly curves of ferroelectrets were also observed by means of piezo-response force microscopy.[124] The acoustic signals only give relative values of the piezoelectric d_{33} coefficients. In order to obtain absolute d_{33} values, dielectric resonance spectroscopy was carried out immediately after the dc voltage cycles. Young's modulus and d_{33} were determined by fitting the real part (inset of Fig. 7(b)) of the measured DRS spectra.[26] Based on the fact that the acoustic signal is proportional to the corresponding d_{33} coefficient, all of the acoustic signals in Fig. 7(a) are converted to piezoelectric d_{33} coefficients. Note that the polarity of d_{33} changes when a phase shift of about 180° occurs between the acoustic signal and the driving ac voltage. Finally, σ_{eff} as a function of V_{dc} can be calculated by using Eq. (7). Figure 7(b) shows that the σ_{eff} versus V_{dc} curves exhibit a hysteresis behavior similar to that of other ferroic materials.

Hysteresis of ferroelectrets has also been investigated by means of a modified Sawyer–Tower circuit. The current under applied charging/poling voltage is given by

$$i = i_{cap} + i_p + i_{cond} = C_s \frac{dV_s}{dt} + A_s \frac{dP_s}{dt} + \frac{V_s}{R_s}, \tag{8}$$

where C_s, V_s, t, A_s, P_s and R_s are sample capacitance, applied voltage, time, sample area, ferroelectric polarization and sample resistance, respectively. The current contains three components resulting from capacitive charging, polarization, and conductivity of the sample. Accordingly, the charge flowing through the circuit during charging can be expressed by

$$\begin{aligned} Q(t) &= Q_{cap}(t) + Q_p(t) + Q_{cond}(t) \\ &= C_s V_s(t) + A_s P_s(t) + \frac{1}{R_s}\int_0^t V_s(t')\mathrm{d}t'. \end{aligned} \tag{9}$$

For ferroelectric polymers, hysteresis loops are usually determined by measuring the poling currents and separating different contributions under specifically designed sinusoidal uni- or bi-polar voltage cycles.[125] However, such a current-voltage scheme is not practical for ferroelectrets because DBDs in cavities of ferroelectrets are very fast processes. Unlike ferroelectric polymers where the poling current varies in the same time scale as the applied poling voltage, DBDs produce current pulses in a time scale of several ns, far beyond the time resolution of the experimental setup. Therefore, a voltage–voltage measurement scheme was proposed for studying the breakdown in thin discharge gaps and the hysteresis behavior of ferroelectrets.[13,126] The inset of Fig. 8 schematically shows the modified Sawyer-Tower circuit used for the measurements. Two standard capacitors much larger than the sample capacitance are connected in series with the sample. The charge flowing through the circuit during the DBDs is obtained by measuring the voltage on the large standard capacitor of 3 nF. Since charging of ferroelectrets often requires voltages of up to several kV, another standard capacitor of 1 μF is employed as a voltage divider that protects the electrometer in case of destructive breakdown in the sample. By applying voltage loops consisting of two positive and then two negative sine-squared semicycles, it

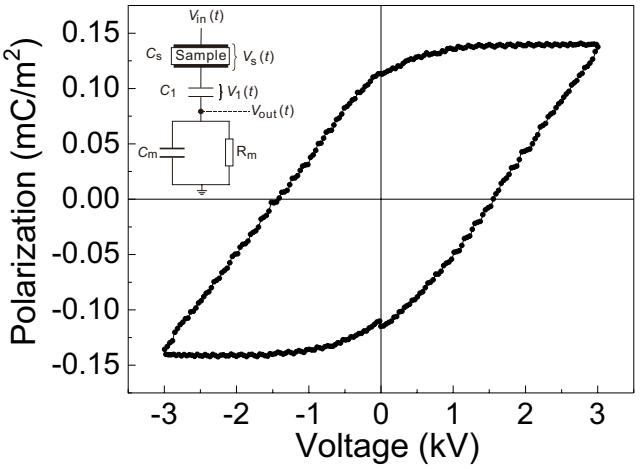

Fig. 8. Polarization as a function of the applied voltage for a tubular-channel FEP ferroelectret. Inset: Schematic view of the circuit used for hysteresis measurements on ferroelectrets in voltage-voltage mode.[13]

is possible to separate different contributions as indicated in Eq. (9). The hysteresis loop of a tubular-channel FEP ferroelectret is displayed in Fig. 8, which demonstrates that DBDs in ferroelectrets result in hysteresis curves that are phenomenologically the same as those of other ferroic materials.

DBD charging of ferroelectrets generates a cold plasma with numerous active species including energetic and reactive charged particles, electrons, and neutral species. Qiu *et al*. reported that repeated DBDs have profound effects on the charging and the resulting piezoelectricity of ferroelectrets.[127–129] DBDs up to 10^3 cycles reduce the threshold charging voltage and hence facilitate the charging process of ferroelectrets. However, the DBD-generated plasma modifies the inner surfaces of the cavities. DBD charging in normal air deteriorates the chargeability of the cavities, leading to severe polarization fatigue. Compared with that of freshly charged samples, the piezoelectric sensitivity and its stability of fatigued samples become much worse even after only 10^3 DBD cycles.

3.2. *Charging methods of high efficiency*

Efficient charging is highly desired in the preparation of ferroelectrets, since the piezoelectric sensitivity is essentially proportional to the effective polarization. Charging methods of high efficiency have been proposed based on improved understanding of the physico-chemical processes during charging of ferroelectrets. According to Paschen's law, the electrical breakdown of a gas is strongly dependant on the type of gas. Paajanen *et al*. implemented corona charging of cellular PP ferroelectrets in a number of dielectric gases.[130,131] Higher corona voltages and/or currents can be achieved with increased ambient gas pressure or with gases of higher dielectric strength, which leads to more efficient charging and larger piezoelectric sensitivity. Particularly, charging in N_2O with atmospheric pressure results in a 70% increase in the piezoelectric d_{33} coefficient of a 70 μm thick cellular PP ferroelectret. By filling the cavities with N_2 gas, d_{33} coefficients of up to 790 pC/N are obtained.

Using two kinds of cellular PP films with different cavity structures and elastic properties, Qiu *et al*. studied the charging efficiency of corona charging in SF_6, a gas widely employed in insulation technology due to its high dielectric strength.[132,133] The penetration of SF_6 was monitored by measuring the thickness of the films. It turned out that the penetration strongly depends on the microstructure of the samples. For the mechanically stiffer cellular PP films (SHD50) with smaller cavity size, penetration of SF_6 was not observed, while for mechanically softer cellular PP films (EUH75) with larger cavity size, penetration of SF_6 was possible with sufficiently long treatment time. Figures 9(a) and 9(b) show the piezoelectric d_{33} coefficient of EUH75 and SHD50 as a function of corona voltages and the corresponding surface potentials in normal laboratory conditions (part I) and in 2 bar SF_6 (part II), respectively.[132] A threshold behavior is clearly seen for corona charging in normal conditions.

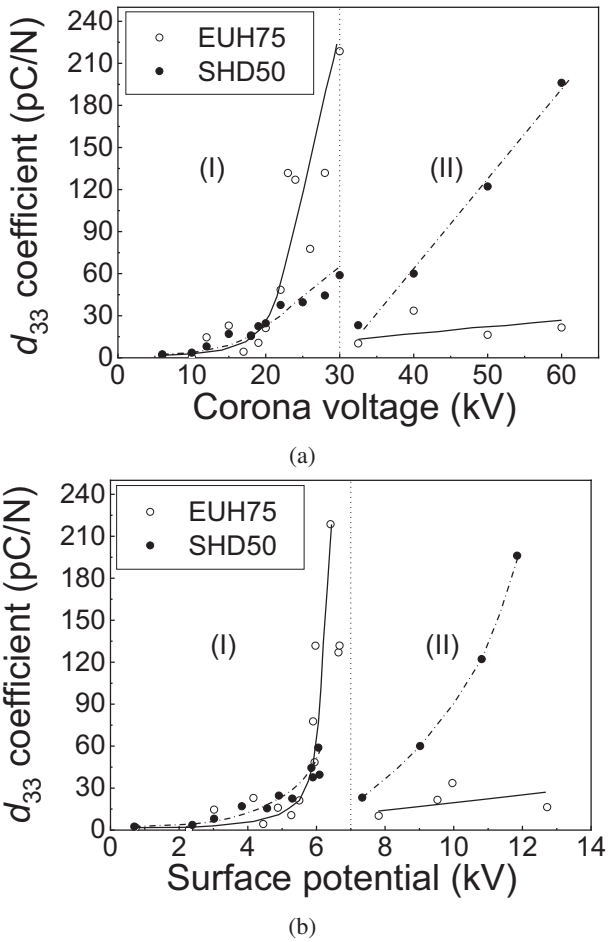

Fig. 9. Piezoelectric d_{33} coefficient as a function of (a) corona voltage and (b) surface potential. Charging conditions: (I) In normal air at atmospheric pressure, (II) In SF_6 at a pressure of 2 bar.[132]

The d_{33} coefficient of EUH75 and SHD50 increases steeply when the corona voltage exceeds 20 kV and 18 kV (surface potential 5.5 and 4.6 kV), respectively. For both EUH75 and SHD50, the d_{33} coefficient does not saturate at the maximum corona voltage of 30 kV in normal air. Higher corona voltage often leads to flash discharge between the corona tip and the sample surface and thus is not practical. In order to further increase the corona voltage, corona charging was carried out in 2 bar SF_6. Such a charging scheme has entirely different effect on EUH75 and SHD50, as can be seen from Fig. 9. The d_{33} of EUH75 is about one order of magnitude lower than the value achieved in normal air, while for SHD50, the d_{33} increases by a factor of three. The big difference is attributed to the microstructure of the samples. EUH75 has large cavities, low density (0.28 g/cm^3) and low Young's modulus (1.35 MPa). During pumping out the normal air and filling with 2 bar SF_6, the air inside the cavities is squeezed out, and the sample thickness decreased by 40%. As the piezoelectricity is very sensitive to the sample thickness,[114,115] the substantial decrease in thickness deteriorates the piezoelectric sensitivity of EUH75. For SHD50 with small cavities, high density (0.53 g/cm^3) and high Young's modulus (6.18 MPa), the microstructure is mainly kept (a thickness change of less than 9%). Consequently, much higher corona voltages and surface potentials in SF_6 result in significantly higher charging efficiency and piezoelectricity. With long enough treatment time (typically several hours), SF_6 can penetrate into the cavities of EUH75, restoring the sample thickness. Corona charging in SF_6 with a tip voltage of 60 kV then also leads to a 1.5 times increase in the d_{33} of EUH75.[133]

As indicated by Eqs. (3) and (4), for easier triggering of the DBD charging in ferroelectrets (i.e., high P_{eff} under the charging voltage), gases with low breakdown strength (thus low V_{th}) are preferred. However, in order to have high remanent polarization (namely, high P_{rem} after the charging voltage is switched off), gases with high breakdown strength (and hence high V_{th}) are desired. Based on this consideration, a charging scheme involving gas exchange was proposed for efficient charging of ferroelectrets.[134] In this method, charging voltage is applied when the cavities are filled with a low-breakdown-strength gas (such as helium at atmospheric pressure). Then, the charging voltage is kept on, and the gas inside the cavities is replaced with a high-breakdown-strength gas (such as nitrogen or atmospheric air). The charging voltage is turned off only after the gas exchange is complete. The proposed method results in much higher charging efficiency for ferroelectrets.

Paschen's law states that the electrical breakdown voltage of a gas gap is a function of pd (Eq. (1)). Therefore, the charging voltage and hence the charging efficiency can be optimized by properly adjusting the gas pressure inside the cavities of ferroelectrets. Figure 10 illustrates the influence of gas pressure during charging on the piezoelectricity of a cellular PP ferroelectret.[43] Penetration of gas moleculars into or out of the cavities is monitored by measuring the sample capacitance that is a function of the thickness. Microstructure

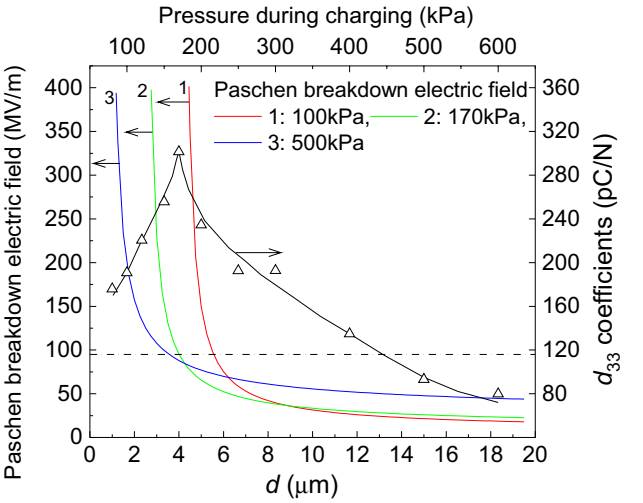

Fig. 10. Bottom X- and left Y-axes: Paschen breakdown field as a function of cavity height d for different gas pressure p as indicated. The dash dot horizontal line indicates the electric field in the cavities at an applied voltage of 6 kV. Top X- and right Y-axes: Piezoelectric d_{33} coefficient as a function of pressure inside the cavities during charging. The line is a guide for the eyes.[43]

analysis of the cross-sectional SEM image shows that a large number of the cavities have a height below 5 μm. At atmospheric pressure, such small cavities have breakdown electric fields higher than the applied electric field at 6 kV (the dash dot horizontal line in Fig. 10), and therefore can not be effectively charged. As the pressure increases, charging of the small cavities is achieved since the breakdown electric field becomes lower than the applied field, which leads to an increase in the d_{33} coefficient. However, as the pressure increases further, the breakdown electric field of large cavities notably increases, resulting in lower charging efficiency of the large cavities. As a result, the d_{33} reaches its maximum at about 170 kPa, and then decreases again as the pressure increases further (Fig. 10).

In addition to pressure, the breakdown electric field of a gas gap is also dependant on gas temperature. Pachen's law holds only at room temperature and needs to be modified at different temperatures. According to the Peek correction, the breakdown electric field of a gas is inversely proportional to the gas temperature.[135] Based on this, a thermal charging scheme, quite similar to the thermal poling method widely used for conventional ferroelectrics, has been proposed for ferroelectrets.[136,137] As schematically shown in Fig. 11, ferroelectrets to be charged are heated up to a suitable elevated temperature so that the threshold voltage becomes lower and the DBDs in the cavities are triggered more easily. In order to have high remanent effective polarization, a high threshold voltage is desired. Therefore, the charging voltage is not switched off until the samples are cooled down to the initial temperature.

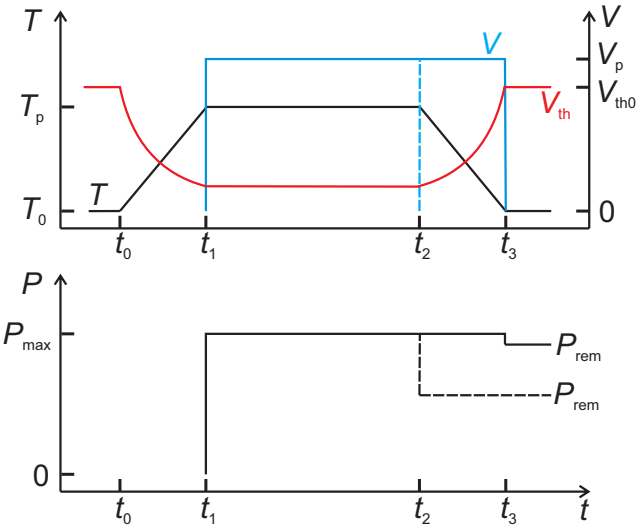

Fig. 11. Thermal poling scheme for ferroelectrets.[137]

In the above-mentioned charging techniques, the applied high voltage triggers the DBDs (micro plasmas) and then drifts the generated charges to the inner surfaces of cavities. Basso *et al*. proposed an AC+DC charging technique in which the high-voltage high-frequency (HV-HF) AC voltage generates plasmas in cavities, while the DC voltage acts as a bias voltage to control the deposition of the charges present in the plasmas.[138] The AC voltage with an amplitude close to the breakdown threshold of the gas in the cavities is enough to create the plasmas. The effective polarization (manifested by the measured piezoelectric coefficient) increases linearly with the DC voltage, and saturates already at the threshold charging voltage of the direct contact charging method. In another charging method, soft X-ray irradiation is employed for photoionization of air molecules inside cavities of ferroelectrets.[139,140] Similarly, a DC voltage is also applied for controlling the charge deposition. Both techniques are quite effective for charging ferroelectrets.

4. Piezeoelectricity of Ferroelectrets

4.1. *Fundamental aspects of the piezoelectric response*

"Piezo" stems from Greek, meaning to squeeze or press. Piezoelectricity is the properties of certain noncentrosymmetrical (without a center of symmetry) materials which are able to convert mechanical signals (strain/displacement or stress/force) into electrical observables (electric displacement/charge or electric field/voltage) and vice versa. In the most general picture, piezoelectricity is observed when a material contains internally separated charges of opposite sign (requirement 1) and exhibits a non-affine mechanical deformation behavior (requirement 2). In addition, a linear relationship between the input and output signals is required.

Figure 12(a) schematically shows the structure and charge distribution of a ferroelectret with cellular structure. Charges

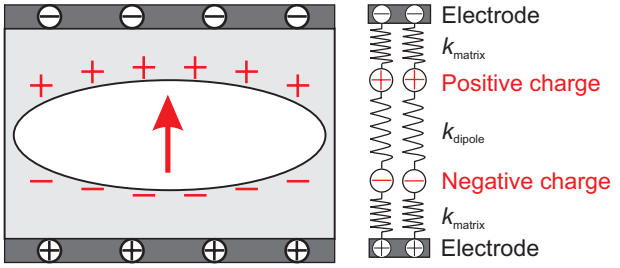

(a) (b)

Fig. 12. (a) Schematic view of cellular ferroelectrets with macroscopic dipoles (internally charged cavities). The piezoelectricity originates from the different elastic behavior of the polymer (matrix phase) and the cavity (dipole phase). (b) Schematic spring-charge model for the occurrence of piezoelectricity in a two-phase material system.

of opposite polarity generated during the DBD charging are trapped on the top and bottom surfaces of cavities, respectively. The charged cavities can be considered as macroscopic dipoles, with a dipole moment $\mu = q.\, l$, where q is the charge and l is the distance between the separated charges, i.e., the cavity height. Along with the macroscopic dipoles, compensating charges are induced on the metal electrodes. The density of the induced charges is directly related and essentially proportional to the density of the macroscopic dipoles (analogous to the polarization in ferroelectrics).

Piezoelectricity can be described by means of various coefficients that correlate mechanical and electrical quantities. For cellular thin-film ferroelectrets, d_{33} is the dominant piezoelectric coefficient due to the special anisotropic material structure. It expresses the ratio of either the charge generated on the surface electrode to the force applied perpendicularly to the film surface (direct piezoelectric effect) or of the change in the film thickness to the voltage applied across the film (inverse piezoelectric effect).

A simplified spring-charge model was proposed to describe the piezoelectric activity of different types of dielectric materials.[12,141] The model consists of a two-phase system with a dipole phase "D" and a matrix phase "M" (Fig. 12(b)). In this context, the dipolar phase has a quite broad meaning. It may consist of intrinsic dipoles in conventional ferroelectrics, internally charged cavities in cellular ferroelectrets, stable interfacial charges (Maxwell–Wagner polarization) in multilayer ferroelectrets, and charges trapped in the material in combination with the induced charges on the electrodes (e.g., in soft/hard double-layer ferroelectrets with single-polarity interfacial charges).

Expressions of the piezoelectric response are determined by theoretical analysis of the model. Considering a thin film or slab poled in the thickness direction, the piezoelectric d_{33} coefficient is given by[141]

$$d_{33} = -\frac{P_3}{Y_M} + \frac{P_3}{Y_D}, \tag{10}$$

where P_3 is the overall remanent polarization, Y_M and Y_D are the elastic modulus of the matrix and the dipole phase, respectively. Equation (10) indicates that the piezoelectric response contains two counteracting contributions, namely, one from the dipole-density effect (the first term in Eq. (10)), and the other from the dipole-moment effect (the second term in Eq. (10)). There exist three situations for dielectric materials or materials systems carrying "dipolar" charges[142]

(i) $k_{matrix} = k_{dipole}$: The matrix and dipole phases have the same elastic modulus (affine deformation), such as in space-charge electrets with isotropic mechanical properties. In this case, piezoelectricity is non-existing.
(ii) $k_{matrix} < k_{dipole}$: The matrix phase is softer than the dipole phase, such as in β-PVDF and copolymers, in composites of polymer with hard particles and of elastomer with polymer granules. The piezoelectricity originates mainly from the dipole density effect (secondary piezoelectricity).
(iii) $k_{matrix} > k_{dipole}$: The matrix phase is stiffer than the dipole phase, such as in ferroelectric ceramics like PZT, in composites of polymers with gases or with liquids. The piezoelectricity originates mainly from the dipole moment effect (primary piezoelectricity).

In ferroelectrets, the gas-filled cavities (dipole phase) are much softer than the polymer walls (matrix phase) between them. Therefore, ferroelectrets exhibit primary piezoelectricity, as typical ferroelectric ceramics do. Ferroelectrets are highly anisotropic materials. Take cellular PP ferroelectrets as examples. The cavities are highly compressible in the thickness direction, whereas in the transverse directions the materials are much stiffer. Consequently, cellular PP ferroelectrets show very large piezoelectric d_{33} coefficients. Values of hundreds of pC/N are often achieved, more than one order of magnitude larger than those found in conventional ferroelectric polymers. The transverse piezoelectric coefficients (d_{31} and d_{32}) of cellular PP ferroelectrets are typically around 2 pC/N, two orders of magnitude lower than the d_{33} coefficient.[26] More recently, ferroelectrets with large transverse piezoelectric activity have also been developed by designing proper sample structures.[143–145]

Equation (10) suggests that for materials with overwhelming secondary or primary piezoelectricity, the ratio of the piezoelectric coefficient d to the remanent polarization P_3 should be approximately equal to the elastic compliance $1/Y_M$ or $1/Y_D$, respectively. Such a dependence is observed for a number of ferroelectrets and ferroelectric polymers.[146] The relationship is also applicable to ferroelectric perovskites when corrected with the tetragonality.[147] The intuitive spring-charge model is very helpful not only for better understanding of existing piezoelectric materials, but also for developing novel piezoelectric materials systems. From the discussions above, it becomes evident that all the existing piezoelectric materials are just examples that fulfill the aforementioned two basic requirements. In practice, the general principles ensure that a material will be piezoelectric if "dipole" and "matrix" phases are artificially engineered into it, leaving a huge space for developing new types of pizoelectric materials.

4.2. *Effect of morphology on the piezoelectricity*

As already mentioned, the piezoelectric properties of ferroelectrets are strongly dependent on the morphology. According to the spring-charge model, large charge density and big difference in the elastic stiffness of different material phases are necessitated in order to have large piezoelectric sensitivity. For cellular polymer ferroelectrets, the size and shape of the cavities can be adjusted by means of gas-diffusion expansion (GDE) treatment.[51–54] For GDE, samples are put into a chamber filled with high-pressure gases (usually dry air or nitrogen). With sufficiently long storage time, the gas molecules diffuse into the cavities, equalizing the internal pressure of the cavities and the ambient pressure in the chamber. Then the pressure in the chamber is suddenly released to atmospheric pressure, and the polymer foams are inflated due to the high internal pressure inside the cavities. The inflated structure is stabilized by heat treatment at elevated temperatures during or right after the pressure treatment.

There are two reasons why inflation through GDE is useful for optimizing the piezoelectric properties of ferroelectrets. First, cavities with proper size have higher charging efficiency. According to Paschen's law, the breakdown electric field increases sharply as the gas gap becomes smaller than about 6 μm (cf. curve 1 in Fig. 10). Very often, cavities spontaneously open up during stretching the polymers that contain tiny mineral particles are in the range of about 1 μm, too flat for efficient charging because the plasma electrons cannot be accelerated sufficiently to ionize the gas molecules. Second, as demonstrated in previous subsections, the piezoelectric activity of ferroelectrets depends on the effective polarization and the elastic modulus. Figure 13 schematically shows the relationships between the structure, elastic and piezoelectric properties of cellular ferroelectrets.[45] Overall, an inversely U-shaped behavior is observed for the piezoelectricity with regard to the sample structures.[45,148–150] Films with small cavities are relatively stiff and therefore show only low piezoelectric activity. Controlled increase of the cavity heights by means of inflation with GDE decreases the elastic stiffness and increases the piezoelectric activity. Further inflation, however, leads to more spherical cavities and a strong increase in the elastic stiffness, which is detrimental to the piezoelectric activity. Such a U-shaped dependence is also confirmed in numerical simulation.[151]

Tuncer *et al*. carried out numerical simulations on two- and three-layer electret systems with uniform and non-uniform charge distributions by coupling the electric field with the stress–strain equations through the Maxwell stress tensor.[152] Various parameters in the model are comprehensively studied regarding their influence on the resulting piezoelectricity. It was shown that non-uniform surface charges and low

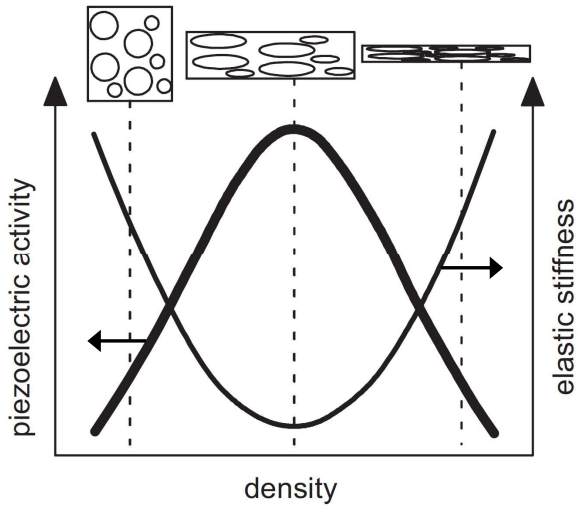

Fig. 13. Schematic dependence of the piezoelectric activity (left ordinate) and the elastic stiffness (right ordinate) of polymer foam ferroelectrets on sample density, and cross sections of the corresponding cellular structures.[45]

Poisson's ratio of material phases lead to high piezoelectric activity. Von Seggern *et al*. studied theoretically and experimentally the charging behavior and the resulting piezoelectricity of three-layer FEP/ePTFE/FEP ferroelectret sandwiches.[82–84] For charging, the important parameters are the thickness ratio of the solid and porous layers as well as the breakdown strength of the porous layer which is dependent on the porosity and thickness of the porous layer. For piezoelectric activity, Young's modulus of the porous layer also plays an important role. These results deepen the understanding of the underlying physics and can be used for optimizing the ferroelectret sandwiches.

As for ferroelectrets with regular cavity structure, the effect of morphology has only been preliminarily investigated in a few works. Altafim *et al*. studied the resonance frequencies of tubular-channel FEP ferroelectrets with different channel geometries.[153,154] Ferroelectret samples with different channel heights or widths show characteristic piezoelectric resonances. These results can be used to develop ferroelectrets with desired resonances or flat resonance regions for specific applications. Ferroelectrets with multi-layer tubular channels have also been studied.[155,156] Samples were fabricated by laminating multi-layer stacks consisting of alternative FEP films and PTFE templates. Channels were created with three arrangements, namely, superimposed, complementary and crossed.[156] Samples with two superimposed channel layers show the highest piezoelectric activity with d_{33} coefficients three times that of samples with a single channel layer. Other arrangements do not lead to noticeable improvement of the piezoelectric activity. Some may even result in lower piezoelectric activity, which is attributed to insufficient charging of the channels and harder sample structures. In general, ferroelectrets with regular cavity structure are fabricated more or less in an empirical manner. Very often the cavity dimensions are 0.5 or 1 mm or so, due probably to the convenience in handling. The effect of morphology should be comprehensively studied as well in order to better the understanding and possibly further improve the performance of this type of ferroelectrets.

4.3. *Stability of the piezoelectricity*

For applications of ferroelectret films, both sensitivity and stability of the piezoelectric activity are important. Stability of cellular PP ferroelectrets has been comprehensively studied in a few papers,[42,157,158] while in many other works, it is often investigated to some extent without being the focus of the study. Above the glass transition temperature of about 10°C, the piezoelectric coefficients of cellular PP ferroelectrets increase with increasing temperature due to a softening of the films. The piezoelectric activity starts to decay irreversibly at temperatures above 60°C, which is ascribed to detrapping of charges captured on the internal surfaces of cavities (Fig. 14). In addition to the thermally-stimulated depolarization, the piezoelectric activity is also influenced

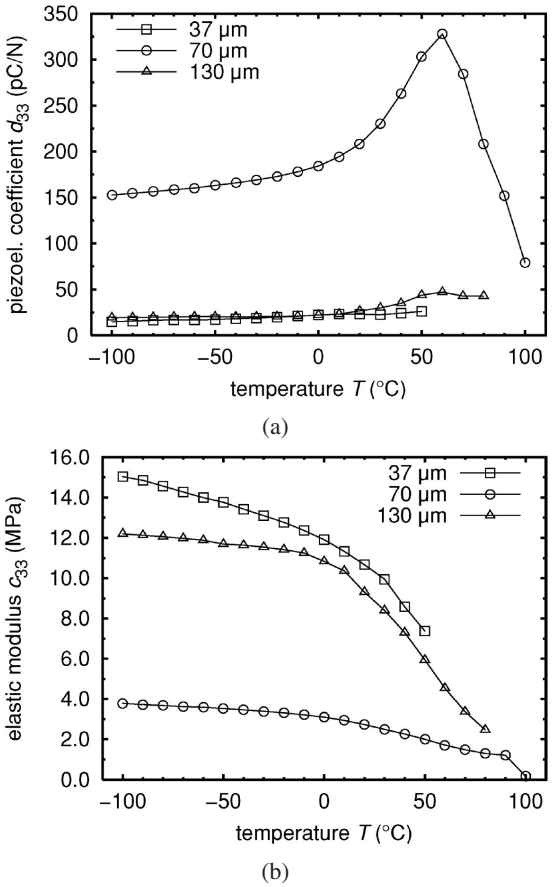

Fig. 14. Piezoelectric d_{33} coefficients (a) and elastic moduli c_{33} (b) as a function of temperature for three different types of cellular PP ferroelectrets. The data were determined from dielectric resonance spectroscopy.[42]

by the instability in the cellular sample structures caused e.g., by gas penetration in varying ambient pressure and/or by pre-loaded mechanical stress.[158] The piezoelectric activity of cellular PP ferroelectrets also decreases upon irradiation with ultraviolet light at wavelengths shorter than 210 nm due to partial photostimulated discharge mostly within the surface layer.[159] However, it was found that the piezoelectric activity of cellular PP ferroelectrets is almost independent of humidity during long-time storage in a humid atmosphere or even in distilled water,[42] coincident with the excellent hydrophobicity and extremely low water-vapor permeability of PP.

Proper chemical modifications are shown to be effective for improving the charge ability of electrets.[160–167] Such approaches are applicable to ferroelectrets since the charges are trapped on the inner surfaces of cavities. Surface modification through gas phase fluorination results in higher sensitivity and thermal stability of the piezoelectric activity of cellular PP ferroelectrets.[168,169] The piezoelectric d_{33} coefficients of the treated samples retain 58% and 45% of the initial values after 151 h and 224 h storage at 70°C and 90°C, 2 and 3 times higher than that of virgin samples, respectively. Modification with suitable chemical solutions either in liquid or in vapor phase is also effective. Rychkov *et al*. carried out a treatment on tubular-channel low-density polyethylene (LDPE) ferroelectrets prepared through the template-based thermal lamination technique[90] with orthophosphoric acid, and achieved an improvement in the thermal stability of the piezoelectric activity by 40 K.[170] Even better results have been achieved through the gas-phase modification of the inner surfaces of the ferroelectret channels using molecular layer deposition technique. In Ref. 171, Rychkov and Altafim treated the inner surfaces of the FEP tubular channels with titanium-tetrachloride vapor to achieve about 100°C improvement in the thermal stability of the piezoelectric coefficients.

Higher stability of the piezoelectricity is achieved by preparing cellular foams from thermally more stable polymers. Cellular polyester ferroelectrets show large piezoelectric activity stable at least up to 80°C.[56–58] COC and FEP are space-charge electrets with outstanding thermal stability, and are also employed for making cellular ferroelectrets. However, it is more difficult to foam and to optimize the cellular structures for more stable base polymers. Both cellular COC and FEP ferroelectrets show relatively low piezoelectric sensitivity.[59,62] In particular, it is quite challenging to fabricate cellular films from fluoropolymers because of their poor mechanical properties and severe creep behavior. Alternatively, ferroelectrets with soft/hard multi-layer structure and with regular cavity structure are created from polymers of high thermal stability. Such ferroelectrets are usually quite soft and may exhibit large piezoelectric activity with a thermal stability up to 120°C or even higher. However, the transducer performance show strong dependence on the mechanical stress due to the high compressibility of the ferroelectret films. Large piezoelectric sensitivity is obtained only at low mechanical stress. Under higher mechanical stress, the samples become stiffer, leading to substantial decreases in their piezoelectric coefficients.[81,87,90] It should be noted that instability of the piezoelectric activity against mechanical stresses exists for all transducer materials. In order to take full advantage of ferroelectrets, their instability must be comprehensively studied. Once the behavior is precisely understood, it can be easily taken into account in many device applications.

5. Applications

Ferroelectrets combine large piezoelectricity and elastic compliance and mechanical flexibility, and therefore are quite promising for a wide range of applications. Several products such as music pick-ups, flexible keyboards, smart bed sensors for health and sleep monitoring (EMfit QSTM) based on cellular PP ferroelectret films (so-called EMFi sensors, where EMFi means electromechanical films) produced by VTT in Finland have already been commercialized. A lot of other applications and device prototypes are being conceived and under investigation in laboratories all over the world, including applications in tactile sensors,[29,30] in health monitoring,[31] in energy harvesting for low-power electronic devices,[32–35] and in air-coupled ultrasonic transducers.[36,37,172] Here, a few representative examples will be discussed to demonstrate the large application potential of ferroelectrets.

Ferroelectret sensors have been studied for potential applications in sensation of robotic hands and health monitoring. Fang *et al*. prepared ferroelectret skin sensors for the acquisition of sensation signal in robotic hands.[173–175] It was found that the ferroelectret sensors can capture and distinguish touching and slipping signals based on the quite different features between these two types of signals, an important functionality for the operation of robotic hands. In Refs. 176 and 177, a ferroelectret-based force myography (FMG) system was developed to record and identify body motions such as different hand and wrist movements. The employed sensors were made of cellular PP ferroelectret films with electrodes on both surfaces. Eight ferroelectret-sensor units were attached at selected positions on the forearm surface (Figs. 15(a) and 15(b)) to form eight-channel FMG maps. In total, eight able-bodied subjects were tested. Six common upper-limb motions as shown in Figs. 15(c)–15(h) were chosen for the study. For each motion, clear eight-channel force signals were recorded by the highly sensitive ferroelectret sensors. The FMG patterns were analyzed to classify the motions. It was shown that evaluation of the FMG patterns by means of linear discriminant analysis and artificial neural network algorithms results in an average motion-classification accuracy of 96.1% and 94.8% for the upperlimb motions, respectively. In addition to body-motion recognition, ferroelectret sensors for health monitoring by detecting physiological pulsatile signals such as heart rate and respiration have been proposed and investigated in a number of studies.[178–181]

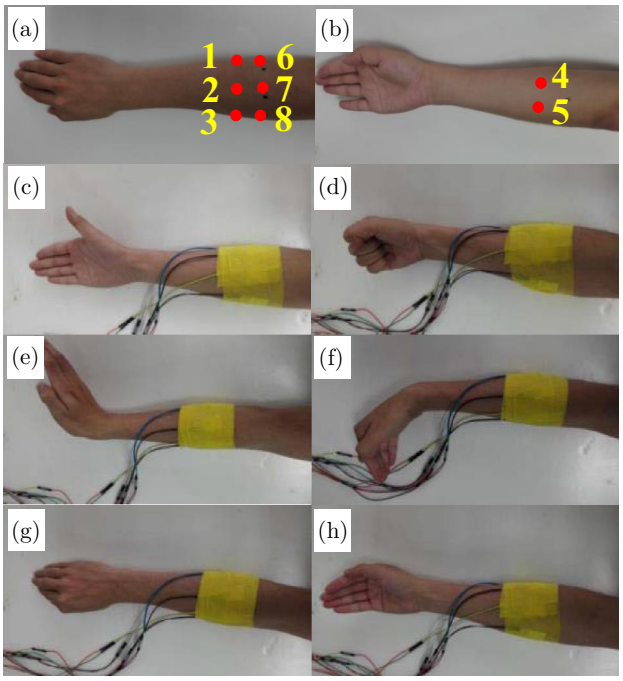

Fig. 15. (a) and (b) Placement of cellular PP ferroelectret sensors. Detection of different body motions using the cellular PP ferroelectret sensors. (c) Hand-opening, (d) Hand-closing, (e) Wrist-extension, (f) Wrist-flexion, (g) Wrist-pronation, and (h) Wrist-supination.[176]

Wirges *et al*. showed that combination of dielectric elastomer actuators (DEAs) and ferroelectrets into a single device may bring forth novel functionalities that are promising for potential applications.[182] A bending actuator was prepared by sandwiching a prestretched DE film with purposely designed flexible and rigid frames. The flexible frame was made of 100 μm thick PET film, having two circular holes with a diameter of 30 mm each and a square hole with a side length of 30 mm, while the rigid one was made of 2 mm thick acryl plate (Fig. 16 top left). Both surfaces of the circular parts of the DE films were metallized with 50 nm thick gold electrodes. Then, the DE film within the square area of the flexible frame was removed, and a tubular-channel FEP ferroelectret was mounted there. Finally, the device was set free, and the central part of the device without rigid frames bended thanks to the elastic energy released by the DE film, forming a self-organized minimum-energy structure that can be used as a bending actuator.[183–185] The actuator unfolds by applying a voltage to the electrodes, and the bending angle decreases with increasing applied voltage. Figure 16 bottom shows that the bending angle is 101 and 60° at an applied voltage of 0 and 2 kV, respectively. It was found that the antiresonance frequency (f_p) of the FEP ferroelectret changes monotonically with the bending angle of the bending actuator. It decreases from 90 to 80 kHz as the applied voltage increases from 0 kV to 2 kV. Therefore, the f_p of ferroelectrets can be employed for *in-situ* monitoring of the actuation of

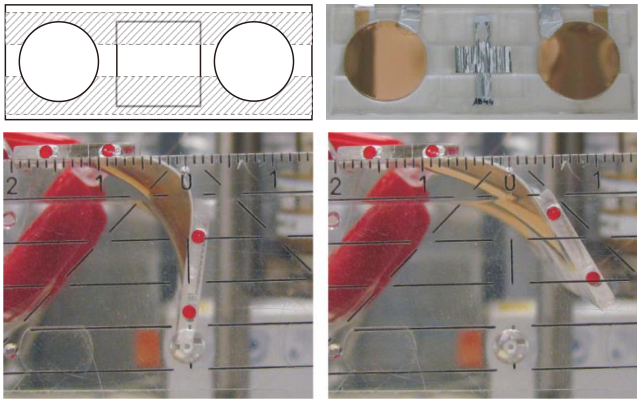

Fig. 16. Top: A self-organized minimum-energy dielectric elastomer actuator. Schematic view of the thin plastic film frame (area constructed with solid lines) and two stiffening pieces (hatched areas enclosed with dashed lines) (left), and a digital photo of a sample (right). Bottom: Digital photos of a minimum-energy bending actuator equipped with an FEP ferroelectret at a driving voltage of 0 kV (left) and 2 kV (right), respectively. The actuator, with two red dots marked on the side of each piece of the stiff frames, was placed behind a goniometer.[182]

DEA devices. On the other hand, the actuation of DEAs can be used for modulating the f_p of ferroelectrets, an important parameter for the application of ferroelectrets. Combination of DEAs and ferroelectrets opens up various new possibilities for applications.

Ferroelectrets show promising potential for electroacoustic applications covering the audio to the ultrasound frequency range. Kodama *et al*. designed a cellular PP piezoelectret-based vibration sensor for acoustic-electric guitars, and studied its performance in comparison with conventional sensors based on PZT.[186] It was shown that only the piezoelectret sensor can detect the vibration of the soundboard over a wide frequency range from 300 Hz to 10 kHz, although its sensitivity is lower than that of PZT sensor. Using piezoelectret sensors, Gidion and Gerhard studied the vibrational properties of a violin during bowing.[187] Two ferroelectret sensors were mounted at the tip and the frog of the violin bow (Fig. 17), and signals from the violin played under

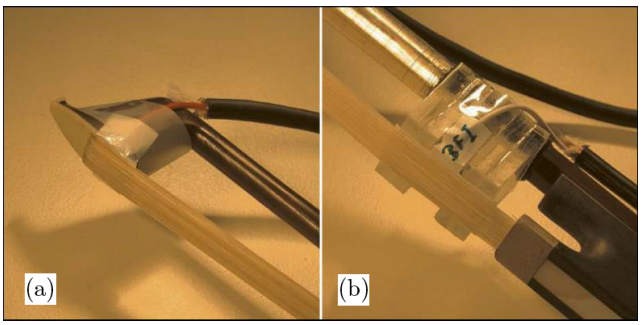

Fig. 17. Cellular PP ferroelectret sensors fixed by bow-hair tension at the tip (a) and near the frog (b) of a violin bow.[187]

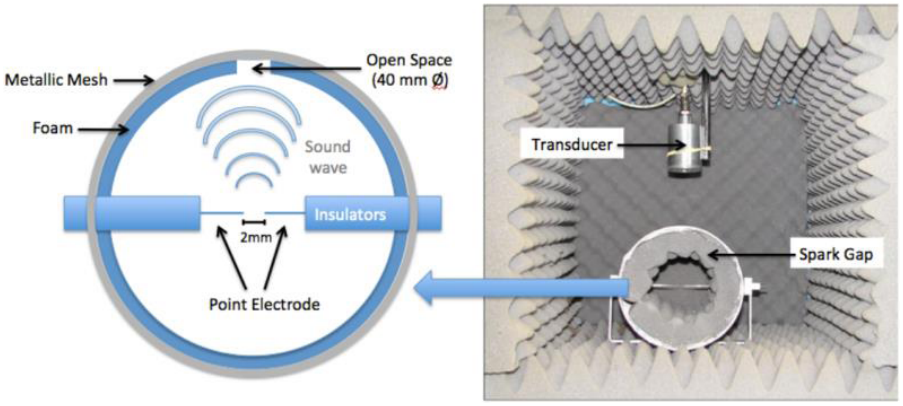

Fig. 18. Schematic view of the point-to-point spark gap device (left), and image of the experimental setup including the ferroelectret transducer and spark gap inside an anechoic chamber.[188]

normal conditions were detected and analysed. From the time-resolved spectra of the signals, the bowed-string harmonics and trends of the longitudinal bow-hair modes are identified. The sensors can also provide vibrotactile input that is valuable for the player-instrument interaction.

Gutnik *et al*. studied the acoustical signatures from partial discharges in a predesigned discharge gap by using ferroelectret sensors.[188] A transducer prototype with a shielded aluminum case was developed by connecting a preamplifier directly to a tubular-channel FEP ferroelectret made through a thermal-lamination technique.[90] The reproducibility of the transducer response was confirmed by sound measurements based on the ASTM E976-10 standard. Partial discharges were generated by means of a 2 mm long point-to-point spark gap, which was mounted inside a cylindrical mesh filled with foam. A circular hole was cut into the foam for the propagation of the acoustic waves from the gas to the transducer (Fig. 18(left)). Partial-discharge measurements were performed firstly inside a cubic anechoic chamber (Fig. 18 (right)). Then, the spark gap was enclosed with an aluminum box (still inside the anechoic chamber) and the transducer was placed onto the box in direct contact. The latter arrangement is more similar with real situations of high-voltage devices. It turns out that the echo resonances of the metal box and the resonances of the ferroelectret sensors strongly influence the recorded signals. Nevertheless, ferroelectret sensors are sensitive enough to detect practical discharges with good reproducibility. Therefore, it is shown that monitoring high-voltage devices such as transformers is another field of application for ferroelectrets. This is a vitally important field since partial discharges can strongly influence the performance and the operating life of high-voltage devices.

6. Conclusions

Nonpolar space-charge polymer foams and polymer-film systems with internally charged cavities (so-called ferroelectrets) are a relatively young class of piezoelectric materials. So far, significant progress has been made in the research and development of ferroelectrets. After the pioneering work on cellular PP ferroelectrets, numerous novel ferroelectrets have been developed using a variety of preparation strategies. In particular, ferroelectrets with well-controlled regular cavity structures have been made of high-performance base polymers such as fluoropolymers. Such ferroelectrets exhibit large and thermally stable piezoelectric sensitivity, and lend themselves easily to laboratory or industrial scale production with good reproducibility.

Charging of ferroelectrets is realized by DBDs inside the cavities and subsequent charge trapping on the internal surfaces. Detailed studies on the charging process by means of optical, electrical and electro-acoustic methods reveal the underlying physics of the threshold charging behavior, polarization saturation, gas ionization during DBDs, and fatigue under repeating voltage cycles. Butterfly curves and polarization-*versus*-electric-field ($P(E)$) hysteresis loops in ferroelectrets are observed through an electroacoustic method together with dielectric resonance spectroscopy. $P(E)$ hysteresis loops are also determined using a modified Sawyer–Tower circuit. These findings not only confirm the "ferroic" behavior of ferroelectrets, but also bring forth charging methods of high efficiency. The internally charged cavities form the "dipole" phase of ferroelectrets. Since the gas-filled cavities are much softer than the polymer walls between them, ferroelectrets possess primary piezoelectric effect (dipole moment effect).

Ferroelectret research will for sure continue to be an active and challenging field. Now, ferroelectrets with outstanding piezoelectric properties are becoming available. In order to take full advantage of these ferroelectrets, influence of the morphology as well as the thermal and mechanical instability of the piezoelectric activity should be comprehensively studied. As the knowledge of ferroelectrets advances, it might even be possible to have custom-made ferroelectrets which can be designed and tuned based on specific applications. There has been constant interest in the application of ferroelectrets because of their excellent overall performance.

More and more attractive applications research, devices prototypes, and eventually more products on the market can be expected in the foreseeable future.

Acknowledgments

Financial support from the National Natural Science Foundation of China (No. 12174102), the National Key Research and Development Program of China (No. 2021YFC3001802), the Shanghai Program for Professor of Special Appointment (Eastern Scholar) at Shanghai Institutions of Higher Learning, and Shanghai Key Laboratory of Special Artificial Microstructure Materials and Technology is gratefully acknowledged.

References

[1]H. Hu, F. Zhang, S. Luo, J. Yue and C. Wang, Electrocaloric effect in relaxor ferroelectric polymer nanocomposites for solid-state cooling, *J. Mater. Chem. A* **8**, 16814 (2020).
[2]A. S. Bhalla, R. Guo and R. Roy, The perovskite structure: A review of its role in ceramic science and technology, *Mater. Res. Innov.* **4**, 3 (2016).
[3]X. Chen, X. Han and Q.-D. Shen, PVDF-based ferroelectric polymers in modern flexible electronics, *Adv. Electron. Mater.* **3**, 1600460 (2017).
[4]W. Xia and Z. Zhang, PVDF-based dielectric polymers and their applications in electronic materials, *IET Nanodielectrics* **1**, 17 (2018).
[5]B. Stadlober, M. Zirkl and M. Irimia-Vladu, Route towards sustainable smart sensors: Ferroelectric polyvinylidene fluoride-based materials and their integration in flexible electronics, *Chem. Soc. Rev.* **48**, 1787 (2019).
[6]E.K. Akdogan, M. Allahverdi and A. Safari, Piezoelectric composites for sensor and actuator applications, *IEEE Trans. Ultrason. Ferroelectr. Freq. Control* **52**, 746 (2005).
[7]A. Jain, K. J. Prashanth, A.K. Sharma, A. Jain and R. Pn, Dielectric and piezoelectric properties of PVDF/PZT composites: A review, *Polym. Eng. Sci.* **55**, 1589 (2015).
[8]L. Gibson and M. Ashby, *Cellular Solids: Structure and Properties*, 2nd edn. (Cambridge University Press, New York, 1999).
[9]G. M. Sessler and R. Gerhard-Multhaupt, *Electrets*, 3rd edn. (Laplacian, Morgan Hill, 1999).
[10]U. Kogelschatz, Dielectric barrier discharges: Their history, discharge physics and industrial applications, *Plasma Chem. Plasma Process* **23**, 1 (2003).
[11]X. Qiu, R. Gerhard and A. Mellinger, Turning polymer foams or polymer-film systems into ferroelectrets: Dielectric barrier discharges in voids, *IEEE Trans. Dielectr. Electr. Insul.* **18**, 34 (2011).
[12]M. Lindner, H. Hoislbauer, R. Schwödiauer, S. Bauer-Gogonea and S. Bauer, Charged cellular polymers with "ferroelectretic" behavior, *IEEE Trans. Dielectr. Electr. Insul.* **11**(2), 255 (2004).
[13]X. Qiu, L. Holländer, W. Wirges, R. Gerhard and H. C. Basso, Direct hysteresis measurements on ferroelectret films by means of a modified Sawyer–Tower circuit, *J. Appl. Phys.* **113**, 224106 (2013).
[14]R. Gerhard-Multhaupt, Less can be more: Holes in polymers lead to a new paradigm of piezoelectric materials for electret transducers, *IEEE Trans. Dielectr. Electr. Insul.* **9**, 850 (2002).
[15]S. Bauer, R. Gerhard-Multhaupt and G. M. Sessler, Ferroelectrets: Soft electroactive foams for transducers, *Phys. Today* **57**(2), 37 (2004).
[16]M. Wegener and W. Wirges, *The Nano-Micro Interface: Bridging the Micro and Nano Worlds*, eds. H.-J. Fecht and M. Werner, Chapter 23 (Wiley-Vch, Weinheim, 2004), pp. 303–317.
[17]M. Wegener and S. Bauer, Microstorms in cellular polymers: A route to soft piezoelectric transducer materials with engineered macroscopic dipoles, *Chem. Phys. Chem.* **6**, 1014 (2005).
[18]X. Qiu, Patterned piezo-, pyro-, and ferroelectricity of poled polymer electrets, *J. Appl. Phys.* **108**, 011101 (2010).
[19]O. Hamdi, F. Mighri and D. Rodrigue, Piezoelectric cellular polymer films: Fabrication, properties and applications, *AIMS Mater. Sci.* **5**(5), 845–869 (2018).
[20]A. Mohebbi, F. Mighri, A. Ajji and D. Rodrigue, Cellular polymer ferroelectret: A review on their development and their piezoelectric properties, *Adv. Polym. Tech.* **37**(2), 21686 (2018).
[21]M. M. A. C. Moreira, I. N. Soares, Y. A. O. Assagra, F. S. I. Sousa, T. M. Nordi, D. M. Dourado, R. H. Gounella, J. P. Carmo, R. A. C. Altafim and R. A. P. Altafim, Piezoelectrets: A brief introduction, *IEEE Sens. J.* **21**(20), 22317 (2021).
[22]I. Graz and A. Mellinger, *Electromechanically Active Polymers*, Polymers and Polymeric Composites: A Reference Series, ed. F. Carpi, Chapter 24 (Springer International Publishing, Switzerland, 2016), pp. 551–560.
[23]X. Qiu, *Electromechanically Active Polymers*, Polymers and Polymeric Composites: A Reference Series, ed. F. Carpi, Chapter 25 (Springer International Publishing, Switzerland, 2016), pp. 561–589.
[24]Y. Wan and Z. Zhong, Effective electromechanical properties of cellular piezoelectret: A review, *Acta Mech. Sin.* **28**(4), 951–959 (2012).
[25]D. Rychkov and R. A. P. Altafim, *Electromechanically Active Polymers*, Polymers and Polymeric Composites: A Reference Series, ed. F. Carpi, Chapter 28 (Springer International Publishing, Switzerland, 2016), pp. 645–659.
[26]A. Mellinger, Dielectric resonance spectroscopy: A versatile tool in the quest for better piezoelectric polymers, *IEEE Trans. Dielectr. Electr. Insul.* **10**, 842 (2003).
[27]P. Fang, L. Holländer, W. Wirges and R. Gerhard, Piezoelectric d_{33} coefficients in foamed and layered polymer piezoelectrets from dynamic mechano-electrical experiments, electro-mechanical resonance spectroscopy and acoustic-transducer measurements, *Meas. Sci. Technol.* **23**, 035604 (2012).
[28]M. Wübbenhorst, X. Zhang and T. Putzeys, *Electromechanically Active Polymers*, Polymers and Polymeric Composites: A Reference Series, ed. F. Carpi, Chapter 26 (Springer International Publishing, Switzerland, 2016), pp. 591–623.
[29]Y. Suzuki and Y. Yasuno, *Electromechanically Active Polymers*, Polymers and Polymeric Composites: A Reference Series, ed. F. Carpi, Chapter 27 (Springer International Publishing, Switzerland, 2016), pp. 625–644.
[30]S. Bauer-Gogonea, S. Bauer, R. Baumgartner, A. Kogler, M. Krause and R. Schwödiauer, *Electromechanically Active Polymers*, Polymers and Polymeric Composites: A Reference Series, ed. F. Carpi, Chapter 29 (Springer International Publishing, Switzerland, 2016), pp. 661–668.
[31]S. Rajala and J. Lekkala, Film-type sensor materials PVDF and EMFi in measurement of cardiorespiratory signals — A review, *IEEE Sens. J.* **12**(3), 439 (2012).
[32]Y. Zhang, C. R. Bowen, S. Kumar Ghosh, D. Mandal, H. Khanbareh, M. Arafa and C. Wan, Ferroelectret materials and devices for energy harvesting applications, *Nano Energy* **57**, 118 (2019).
[33]X. Mo, H. Zhou, W. Li, Z. Xu, J.g Duan, L. Huang, B. Hu and J. Zhou, Piezoelectrets for wearable energy harvesters and sensors, *Nano Energy* **65**, 104033 (2019).
[34]X. Zhang, H.z von Seggern, G. M. Sessler and M. Kupnik, Mechanical energy harvesting with ferroelectrets, *IEEE Electr. Insul. M* **36**(6), 47 (2020).

[35]M. A. Ansari and P. Somdee, Piezoelectric polymeric foams as flexible energy harvesters: A review, *Adv. Energy Sustainability Res.* **3**(9), 2200063 (2022).
[36]M. Gaal, D. Kotschate and K. Bente, Advances in air-coupled ultrasonic transducers for non-destructive testing, *Proc. Mtgs. Acoust.* **38**, 030003 (2019).
[37]W. Essig, Y. Bernhardt, D. Döring, I. Solodov, T. Gautzsch, M. Gaal, D. Hufschläger, R. Sommerhuber, M. Brauns, T. Marhenke, J. Hasener, A. Szewieczek and W. Hillger, Air-coupled ultrasound emerging NDT method, *ZfP-Zeitung.* **173**, 32 (2021).
[38]C. Hennion and J. Lewiner, A new principle for the design of condenser electret transducers, *J. Acoust. Soc. Am.* **63**(4), 1229 (1978).
[39]K. Kirjavainen, Electromechanical film and procedure for manufacturing same, U.S. Patent No. 4 654 546, 1987.
[40]A. Savolainen and K. Kirjavainen, Electrothermomechanical film. Part I. Design and characteristics, *J. Macromol. Sci. Chem.* **A26**, 583 (1989).
[41]J. Backman, Audio applications of electrothermomechanical film (ETMF), *J. Audio Eng. Soc.* **38**(5), 364 (1990).
[42]A. Mellinger, M. Wegener, W. Wirges, R. R. Mallepally and R. Gerhard-Multhaupt, Thermal and temporal stability of ferroelectret films made from cellular polypropylene/air composites, *Ferroelectrics* **331**, 189 (2006).
[43]X. Qiu, A. Mellinger and R. Gerhard, Influence of gas pressure in the voids during charging on the piezoelectricity of ferroelectrets, *Appl. Phys. Lett.* **92**, 052901 (2008).
[44]A. Mellinger, M. Wegener, W. Wirges and R. Gerhard-Multhaupt, Thermally stable dynamic piezoelectricity in sandwich films of porous and non-porous amorphous fluoropolymer, *Appl. Phys. Lett.* **79**, 1852 (2001).
[45]M. Wegener, W. Wirges and R. Gerhard-Multhaupt, Piezoelectric polyethylene terephthalate (PETP) foams specifically designed and prepared ferroelectret films, *Adv. Eng. Mater.* **7**, 1128 (2005).
[46]M. Wegener, W. Wirges, J. P. Dietrich and R. Gerhard-Multhaupt, Polyethylene therephthalate (PETP) foams as ferroelectrets, *Proc. 12th Int. Symp. Electrets* (2005), pp. 28–30.
[47]W. Wirges, M. Wegener, O. Voronina, L. Zirkel and R. Gerhard-Multhaupt, Optimized preparation of elastically soft, highly piezoelectric, cellular ferroelectrets from nonvoided poly(ethylene terephthalate) films, *Adv. Funct. Mater.* **17**, 324 (2007).
[48]A. I. Cooper, Porous materials and supercritical fluids, *Adv. Mater.* **15**(13), 1049 (2003).
[49]S. P. Nalawade, F. Picchioni and L. Janssen, Supercritical carbon dioxide as a green solvent for processing polymer melts: Processing aspects and applications, *Prog. Polym. Sci.* **31**, 19 (2006).
[50]M. A. Jacobs, Measurement and modeling of thermodynamic properties for the processing of polymers in supercritical fluids, Ph.D. Thesis (Technische Universiteit Eindhoven, 2004).
[51]M. Paajanen, H. Minkkinen, and J. Raukola, Gas diffusion expansion-increased thickness and enhanced electromechanical response of cellular polymer electret films, *Proc. 11th Int. Symp. Electrets* (2002), pp. 191–194.
[52]M. Wegener, W. Wirges, R. Gerhard-Multhaupt, M. Paajanen, H. Minkkinen and J. Raukola, Enhancing the cellular structure and the electromechanical response of ferroelectrets — gas diffusion expansion of voided polypropylene films, *Annual Report IEEE Conf. Electric Insulation and Dielectric Phenomena* (2003), pp. 36–39.
[53]M. Wegener, W. Wirges, J. Fohlmeister, B. Tiersch and R. Gerhard-Multhaupt, Two-step inflation of cellular polypropylene films: Void-thickness increase and enhanced electromechanical properties, *J. Phys. D Appl. Phys.* **37**, 623 (2004).
[54]X. Zhang, J. Hillenbrand and G. M. Sessler, Piezoelectric d_{33} coefficient of cellular polypropylene subjected to expansion by pressure treatment, *Appl. Phys. Lett.* **85**, 1226 (2004).
[55]X. Qiu, Z. Xia and F. Wang, The storage and its stability of space charge in poly(ethylene naphthalene-2, 6-dicarboxylate), *Sci. China Ser. E* **49**(1), 1 (2006).
[56]P. Fang, M. Wegener, W. Wirges, R. Gerhard and L. Zirkel, Cellular polyethylene-naphthalate ferroelectrets: Foaming in supercritical carbon dioxide, structural and electrical preparation, and resulting piezoelectricity, *Appl. Phys. Lett.* **90**, 192908 (2007).
[57]P. Fang, W. Wirges, M. Wegener, L. Zirkel and R. Gerhard, Cellular polyethylene-naphthalate films for ferroelectret applications: Foaming, inflation and stretching, assessment of electromechanically relevant structural features, *E-Polymers* **8**(1), 43 (2008).
[58]P. Fang, X. Qiu, W. Wirges, R. Gerhard and L. Zirkel, Polyethylene-naphthalate (PEN) ferroelectrets: Cellular structure, piezoelectricity and thermal stability, *IEEE Trans. Dielectr. Electr. Insul.* **17**, 1079 (2010).
[59]O. Voronina, M. Wegener, W. Wirges, R. Gerhard, L. Zirkel and H. Münstedt, Physical foaming of fluorinated ethylene-propylene (FEP) copolymers in supercritical carbon dioxide: Single film fluoropolymer piezoelectrets, *Appl. Phys. A Mater.* **90**, 615 (2008).
[60]G. M. Sessler, G. M. Yang and W. Hatke, Electret properties of cycloolefin copolymers. Electrical insulation and dielectric phenomena, *Annual Report IEEE Conf. Electrical Insulation Dielectric Phenomena* (1997), pp. 467–470.
[61]M. Wegener, M. Paajanen, O. Voronina, R. Schulze, W. Wirges and R. Gerhard-Multhaupt, Voided cyclo-olefin polymer films: Ferroelectrets with high thermal stability, *Proc. 12th Int. Symp. Electrets* (2005), pp. 47–50.
[62]E. Saarimäki, M. Paajanen, A. Savijärvi, H. Minkkinen, M. Wegener, O. Voronina, R. Schulze, W. Wirges and R. GerhardMulthaupt, Novel heat durable electromechanical film: Processing for electromechanical and electret applications, *IEEE Trans. Dielectr. Electr. Insul.* **13**(5), 963 (2006).
[63]Z. Xia, R. Gerhard-Multhaupt, W. Künstler, A. Wedel and R. Danz, High surface-charge stability of porous polytetrafluoroethylene electret films at room and elevated temperatures, *J. Phys. D Appl. Phys.* **32**, L83 (1999).
[64]X. Qiu, Z. Xia, F. Wang, W. Wirges and R. Gerhard, Influence of thermal treatment on the charge stability of non-porous and porous polytetrafluoroethylene (PTFE) film electrets, *Proc. Int. Conf. Solid Dielectric* (2010).
[65]Z. Xia, S. Ma, X. Qiu and Y. Zhang, Thermal stability of piezoelectricity for porous polytetrafluoroethylene electret film, *J. Electrostat.* **58**, 265 (2003).
[66]Z. Xia, S. Ma, X. Qiu, Y. Wu and F. Wang, Influence of porosity on the stability of charge and piezoelectricity for porous polytetrafluoroethylene film electrets, *J. Electrostat.* **59**, 57 (2003).
[67]Z. Xia, S. Ma, J. Zhu, X. Qiu, Y. Zhang, R. Gerhard-Multhaupt and W. Künstler, Piezoelectric activity and its stability of polytetrafluoroethylene (PTFE) films, *Acta Phys. Sin.* **52**, 2075 (2003).
[68]M. Wegener, W. Wirges and B. Tiersch, Porous polytetrafluoroethylene (PTFE) electret films: Porosity and time dependent charging behavior of the free surface, *J. Porous Mater.* **14**, 111 (2007).
[69]M. Wegener, W. Wirges, M. Paajanen and R. Gerhard, Charging behavior and thermal stability of porous and non-porous polytetrafluoroethylene (PTFE) electrets, *Annual Report IEEE Conf. Electric Insulation and Dielectric Phenomena* (2007), pp. 449– 452.
[70]R. Gerhard-Multhaupt, M. Wegener, W. Künstler, W. Wirges, T. Görne, K. Urayama and D. Neher, Inverse piezoelectricity of porous PTFE films with bipolar space charge, *Annual Report IEEE Conf. Electric Insulation and. Dielectric Phenomena* (2000), pp. 377–380.
[71]R. Gerhard-Multhaupt, W. Künstler, T. Görne, A. Pucher, T. Weinhold, M. Seiss, Z. Xia, A. Wedel and R. Danz, Porous polytetrafluoroethylene space-charge electrets for piezoelectrical applications, *IEEE Trans. Dielectr. Electr. Insul.* **7**, 480 (2000).

[72]T. Weinhold, M. Seiss, W. Künstler, T. Görne and R. Gerhard-Multhaupt, Porous polytetrafluoroethylene (PTFE) single-film space-charge electrets with high piezoelectric coefficients, *8th Int. Conf. Dielectric Materials, Measurements and Applications (IEE Conf. Publ. No. 473)* (2000), pp. 380–385.
[73]R. Kacprzyk, E. Motyl, J. B. Gajewski and A. Pasternak, Piezoelectric properties of nonuniform electrets, *J. Electrost.* **35**(2–3), 161 (1995).
[74]R. Kacprzyk, A. Dobrucki and J. B. Gajewski, Double-layer electret transducer, *J. Electros.* **39**(1), 33 (1997).
[75]R. Gerhard-Multhaupt, Z. Xia, W. Künstler and A. Pucher, Preliminary study of multi-layer space-charge electrets with piezoelectric properties from porous and non-porous Teflon films, *Proc. 10th Int. Symp. Electrets* (1999), pp. 273–276.
[76]W. Künstler, Z. Xia, T. Weinhold, A. Pucher and R. Gerhard-Multhaupt, Piezoelectricity of porous polytetrafluoroethylene singleand multiple-film electrets containing high charge densities of both polarities, *Appl. Phys. A Mater.* **70**, 5 (2000).
[77]M. Wegener, W. Wirges, K. Richter, W. Künstler and R. Gerhard-Multhaupt, Charge stability and piezoelectric properties of porous fluoropolymer space-charge electrets in layer systems, *Proc. 4th Int. Conf. Electric Charges in Non-Conductive Materials* (2001), pp. 257–260.
[78]M. Wegener, W. Wirges, W. Künstler, R. Gerhard-Multhaupt, B. Elling, M. Pinnow and R. Danz, Coating of porous polytetrafluoroethylene films with other polymers for electret applications, *Annual Report IEEE Conf. Electric Insulation and Dielectric Phenomena* (2001), pp. 100–103.
[79]R. Schwödiauer, G.S. Neugschwandtner, K. Schrattbauer, M. Lindner, M. Vieytes, S. Bauer-Gogonea and S. Bauer, Preparation and characterization of novel piezoelectric and pyroelectric polymer electrets, *IEEE Trans. Dielect. Electr. Insul.* **7**, 578 (2000).
[80]R. Schwödiauer, G. S. Neugschwandtner, S. Bauer-Gogonea, S. Bauer and W. Wirges, Low-dielectric-constant cross-linking polymers: Film electrets with excellent charge stability, *Appl. Phys. Lett.* **75**(25), 3998 (1999).
[81]Z. Hu and H. von Seggern, Breakdown-induced polarization buildup in porous fluoropolymer sandwiches: A thermally stable piezoelectret, *J. Appl. Phys.* **99**, 024102 (2006).
[82]H. von Seggern, S. Zhukov and S. N. Fedosov, Poling dynamics and thermal stability of FEP/ePTFE/FEP sandwiches, *IEEE Trans. Dielectr. Electr. Insul.* **17**(4), 1056 (2010).
[83]H. von Seggern, S. Zhukov and S. Fedosov, Importance of geometry and breakdown field on the piezoelectric d_{33} coefficient of corona charged ferroelectret sandwiches, *IEEE Trans. Dielectr. Electr. Insul.* **18**(1), 49 (2011).
[84]S. Zhukov, S. Fedosov and H. von Seggern, Piezoelectrets from sandwiched porous polytetrafluoroethylene (ePTFE) films: Influence of porosity and geometry on charging properties, *J. Phys. D: Appl. Phys.* **44**, 105501 (2011).
[85]J. Huang, X. Zhang, Z. Xia and X. Wang, Piezoelectrets from laminated sandwiches of porous polytetrafluoroethylene films and nonporous fluoroethylenepropylene films, *J. Appl. Phys.* **103**, 084111 (2008).
[86]X. Zhang, X. Wang, G. Cao, D. Pan and Z. Xia, Polytetrafluoroethylene piezoelectrets prepared by sintering process, *Appl. Phys. A: Mater. Sci. Process.* **97**, 859 (2009).
[87]X. Zhang, X. Zhang, G. M. Sessler and X. Gong, Quasi-static and dynamic piezoelectric responses of layered polytetrafluoroethylene ferroelectrets, *J. Phys. D Appl. Phys.* **47**, 015501 (2014).
[88]R. A. C. Altafim, H. C. Basso, R. A. P. Altafim, L. Lima, C. V. de Aquino, L. Goncalves Neto and R. Gerhard-Multhaupt, Piezoelectrets from thermo-formed bubble structures of fluoropolymerelectret films, *IEEE Trans. Dielectr. Electr. Insul.* **13**(5), 979 (2006).
[89]H. C. Basso, R. A. P. Altafilm, R. A. C. Altafilm, A. Mellinger, P. Fang, W. Wirges and R. Gerhard, Three-layer ferroelectrets from perforated Teflon-PTFE films fused between two homogeneous Teflon-FEP films, *Annual Report IEEE Conf. Electrical Insulation and Dielectric Phenomena* (2007), pp. 453–456.
[90]R. A. P. Altafim, X. Qiu, W. Wirges, R. Gerhard, R. A. C. Altafim, H. C. Basso, W. Jenninger and J. Wagner, Template-based fluoroethylenepropylene piezoelectrets with tubular channels for transducer applications, *J. Appl. Phys.* **106**, 014106 (2009).
[91]R. A. P. Altafim, D. Rychkov, W. Wirges, R. Gerhard, H. C. Basso, R. A. C. Altafim and M. Melzer, Laminated tubular-channel ferroelectret systems from low-density polyethylene films and from fluoroethylene-propylene copolymer films — A comparison, *IEEE Trans. Dielectr. Electr. Insul.* **19**(4), 1116 (2012).
[92]R. Altafim, Y. Assagra, R. Altafim, J. Carmo, T. Palitó, A. Santos and D. Rychkov, Piezoelectric-magnetic behavior of ferroelectrets coated with magnetic layer, *Appl. Phys. Lett.* **119**, 241901 (2021).
[93]X. Zhang, J. Hillenbrand and G. M. Sessler, Thermally stable fluorocarbon ferroelectrets with high piezoelectric coefficient, *Appl. Phys. A Mater.* **84**, 139 (2006).
[94]X. Zhang, J. Hillenbrand and G. M. Sessler, Ferroelectrets with improved thermal stability made from fused fluorocarbon layers, *J. Appl. Phys.* **101**, 054114 (2007).
[95]D. R. Falconi, R. A. C. Altafim, H. C. Basso, R. A. P. Altafim, W. Wirges and R. Gerhard, Piezoelectric sensor based on electrets thermoforming technology, *Proc. Int. Conf. Solid Dielectrics* (2010), pp. 1-3, DOI: 10.1109/ICSD.2010.5568029.
[96]X. Zhang, G. Cao, Z. Sun and Z. Xia, Fabrication of fluoropolymer piezoelectrets by using rigid template: Structure and thermal stability, *J. Appl. Phys.* **108**, 064113 (2010).
[97]Z. Sun, X. Zhang, Z. Xia, X. Qiu, W. Wirges, R. Gerhard, C. Zeng, C. Zhang and B. Wang, Polarization and piezoelectricity in polymer films with artificial void structure, *Appl. Phys. A Mater.* **105**, 197 (2011).
[98]X. Zhang, J. Hillenbrand, G. M. Sessler G M, S. Haberzettl and K. Lou, Fluoroethylenepropylene ferroelectrets with patterned microstructure and high, thermally stable piezoelectricity, *Appl. Phys. A Mater.* **107**, 621 (2012).
[99]P. Fang, F. Wang, W. Wirges, R. Gerhard and H. C. Basso, Three-layer piezoelectrets from fluorinated ethylene-propylene (FEP) copolymer films, *Appl. Phys. A Mater.* **103**, 455 (2011).
[100]X. Qiu, L. Holländer, R. F. Suárez, W. Wirges and R. Gerhard, Polarization from dielectric-barrier discharges in ferroelectrets: Mapping of the electric-field profiles by means of thermalpulse tomography, *Appl. Phys. Lett.* **97**, 072905 (2010).
[101]D. Rychkov, R. A. P. Altafim and R. Gerhard, Unipolar ferroelectrets — Following the example of the electret microphone more closely, *Annual Reports IEEE Conf. Electrical Insulation and Dielectric Phenomena* (2014), pp. 860–862.
[102]M. Sborikas, X. Qiu, W. Wirges, R. Gerhard, W. Jenninger and D. Lovera, Screen printing for producing ferroelectret systems with polymer-electret films and well-defined cavities, *Appl. Phys. A Mater.* **114**, 515 (2014).
[103]Y. A. O. Assagra, R. A. P. Altafim, R. A. C. Altafim and J. P. Carmo, Piezoelectrets with well-defined cavities produced from 3D-printed ABS structures, *Electron. Lett.* **51**(24), 2028 (2015).
[104]I. Kierzewski, S. S. Bedair, B. Hanrahan, H. Tsang, L. Hu and N. Lazarus, Adding an electroactive response to 3D printed materials: Printing a piezoelectret, *Addit. Manuf.* **31**, 100963 (2020).
[105]T. T. C. Palitó, Y. A. O. Assagra, R. A. P. Altafim, J. P. Carmo and R. A. C. Altafim, Hydrophone based on 3D printed polypropylene (PP) piezoelectret, *Electron. Lett.* **55**(4), 203 (2019).
[106]Y. A. O. Assagra, R. A. P. Altafim, J. P. do Carmo, R. A. C. Altafim, D. Rychkov, W. Wirges and R. Gerhard, A new route to

piezo-polymer transducers: 3D printing of polypropylene ferroelectrets, *IEEE Trans. Dielectr. Electr. Insul.* **27**(5), 1668 (2020).
[107]Y. Li and C. Zeng, Low-temperature CO_2-assisted assembly of cyclic olefin copolymer ferroelectrets of high piezoelectricity and thermal stability, *Macromol. Chem. Phys.* **214**, 2733 (2013).
[108]J. Wang, T. Hsu, C. Yeh, J. Tsai and Y. Su, Piezoelectric polydimethylsiloxane films for MEMS transducers, *J. Micromech. Microeng.* **22**, 015013 (2012).
[109]J. Wang, J. Tsai and Y. Su, Piezoelectric rubber films for highly sensitive impact measurement, *J. Micromech. Microeng.* **23**, 075009 (2013).
[110]M. Lindner, S. Bauer-Gogonea and S. Bauer, Dielectric barrier microdischarges: Mechanism for the charging of cellular piezoelectric polymers, *J. Appl. Phys.* **91**(8), 5283 (2002).
[111]A. Mellinger and O. Mellinger, Breakdown threshold of dielectric barrier discharges in ferroelectrets: Where Paschen's law fails, *IEEE Trans. Dielectr. Electr. Insul.* **18**, 43 (2011).
[112]M. Wegener, M. Paajanen, W. Wirges and R. Gerhard-Multhaupt, Corona-induced partial discharges, internal charge separation and electromechanical transducer properties in cellular polymer films, *Proc. 11th Int. Symp. Electrets* (2002), pp. 54–57.
[113]R. Gerhard-Multhaupt, M. Wegener, W. Wirges, J. A. Giacometti, R. A. C. Altafim, L. F. Santos, R. M. Faria and M. Paajanen, Electrode poling of cellular polypropylene films with short high-voltage pulses, *Annual Reports. IEEE Conf. Electrical Insulation and Dielectric Phenomena* (2002), pp. 299–302.
[114]G. M. Sessler and J. Hillenbrand, Electromechanical response of cellular electret films, *Appl. Phys. Lett.* **75**, 3405 (1999).
[115]M. Paajanen, H. Välimäki, and J. Lekkala, Modeling the sensor and actuator operations of the electromechanical film EMFi, *IEEE 10th Int. Symp. Electrets, IEEE Service Center,* Piscataway, NJ, USA (1999), pp. 735–738.
[116]P. Zhang, Z. Xia, X. Qiu, F. Wang and X. Y. Wu, Influence of charging parameters on piezoelectricity for cellular polypropylene film electrets, *IEEE 12th Int. Symp. Electrets, IEEE Service Center*, Piscataway, NJ (2005), pp. 39–42.
[117]S. Zhukov and H. von Seggern, Polarization hysteresis and piezoelectricity in open-porous fluoropolymer sandwiches, *J. Appl. Phys.* **102**, 044109 (2007).
[118]X. Qiu, A. Mellinger, M. Wegener, W. Wirges and R. Gerhard, Barrier discharges in cellular polypropylene ferroelectrets: How do they influence the electromechanical properties? *J. Appl. Phys.* **107**, 104112 (2007).
[119]X. Qiu, A. Mellinger, W. Wirges and R. Gerhard, Spectroscopic study of dielectric barrier discharges in cellular polypropylene ferroelectrets, *Appl. Phys. Lett.* **91**, 132905 (2007).
[120]X. Qiu, A. Mellinger, W. Wirges, R. Gerhard, E. Aubert, G. Teyssedre, A. Petre, and C. Laurent, Light Emission from Cellular Polypropylene Ferroelectrets under High Electric Fields and Its Correlation with Piezoelectricity, *IEEE 13th Int. Sym. Electrets ISE 13* (2008), C205–C205. doi: 10.1109/ISE.2008.4814078.
[121]R. A. P. Altafim, H. C. Basso, R. A. C. Altafim, X. Qiu, W. Wirges and R. Gerhard, Discharge patterns in three-layer ferroelectret systems with perforated polymer films, *IEEE 13th Int. Symp. Electrets ISE 13* (2008), C202–C202, doi:10.1109/ise.2008.4814075.
[122]R. A. C. Altafim, R. A. P. Altafim, H. C. Basso, X. Qiu, W. Wirges, R. Gerhard, W. Jenninger and J. Wagner, Dielectric barrier discharges in multi-layer polymer ferroelectrets, *Annual Reports IEEE Conf. Electrical Insulation and Dielectric Phenomena* (2009), pp. 142–145, doi: 10.1109/CEIDP.2009.5377827.
[123]X. Qiu, R. Gerhard and A. Mellinger, In-situ acoustical investigation of the polarization build-up in cellular polypropylene ferroelectrets, *IEEE Trans. Dielectr. Electr. Insul.* **17**, 1043 (2010).
[124]H. Miao, Y. Sun, X. Zhou, Xilong, Y. Li and F. Li, Piezoelectricity and ferroelectricity of cellular polypropylene electrets films characterized by piezoresponse force microscopy, *J. Appl. Phys.* **116** (6), 066820 (2014).
[125]M. Wegener, Polarization-electric field hysteresis of ferroelectric PVDF films: Comparison of different measurement regimes, *Rev. Sci. Instrum.* **79**, 106103 (2008).
[126]H. C. Basso, X. Qiu, W. Wirges and R. Gerhard, Temporal evolution of the re-breakdown voltage in small gaps from nanoseconds to milliseconds, *Appl. Phys. Lett.* **102**, 012904 (2013).
[127]X. Qiu and R. Gerhard, Effective polarization fatigue from repeated dielectric barrierdischarges in cellular polypropylene ferroelectrets, *Appl. Phys. Lett.* **93**, 152902 (2008).
[128]X. Qiu, W. Wirges and R. Gerhard, Beneficial and detrimental fatigue effects of dielectric barrier discharges on the piezoelectricity of polypropylene ferroelectrets, *J. Appl. Phys.* **110**, 024108 (2011).
[129]X. Qiu, M. Sborikas, W. Wirges and R. Gerhard, Fatigue and recovery of cellular-polypropylene piezoelectrets during and after dielectric-barrier discharges, *Annual Reports IEEE Conf. Electrical Insulation and Dielectric Phenomena* (2013), pp. 591–594.
[130]M. Paajanen, M. Wegener and R. Gerhard-Multhaupt, Charging of cellular space-charge electret films in various gas atmospheres, *Annual Reports IEEE Conf. Electrical Insulation and Dielectric Phenomena* (2001), pp. 24–27.
[131]M. Paajanen, M. Wegener and R. Gerhard-Multhaupt, Understanding the role of the gas in the voids during corona charging of cellular electret films — a way to enhance their piezoelectricity, *J. Phys. D Appl. Phys.* **34**, 2482 (2001).
[132]X. Qiu, Z. Xia, Z. An and X. Wu, The piezoelectricity of heat-expanded PP cellular electret, *Acta Phys. Sin.* **54**(1), 402 (2005).
[133]X. Qiu, M. Wegener, W. Wirges, X. Zhang, J. Hillenbrand, Z. Xia, R. Gerhard-Multhaupt and G. M. Sessler, Penetration of sulfur hexafluoride into cellular polypropylene films and its effect on the electric charging and electromechanical response of ferroelectrets, *J. Phys. D Appl. Phys.* **38**, 649 (2005).
[134]X. Qiu, Significant enhancement of the charging efficiency in the cavities of ferroelectrets through gas exchange during charging, *Appl. Phys. Lett.* **109**, 222903 (2016).
[135]F. W. Peek, *Dielectric Phenomena in High Voltage Engineering* (McGraw-Hill Book Company, New York, 1915, 1920, and 1929).
[136]X. Qiu, M. Steffen, W. Wirges and R. Gerhard, Temperature dependence of quasi-ferroelectric hysteresis in a model ferroelectret system, *Annual Reports IEEE Conf. Electrical Insulation and Dielectric Phenomena* (2015), pp. 644–647.
[137]X. Qiu, W. Wirges and R. Gerhard, Thermal poling of ferroelectrets: How does the gas temperature influence dielectric barrier discharges in cavities? *Appl. Phys. Lett.* **108**, 252901 (2016).
[138]H. C. Basso, J. R. B. de A Monteiro, D. B. Mazulquim, G. T. de Paula, L. G. Neto and R. Gerhard, Alternating current-generated plasma discharges for the controlled direct current charging of ferroelectrets, *J. Appl. Phys.* **114** (10), 104101 (2013).
[139]Y. Feng, K. Hagiwara, Y. Iguchi and Y. Suzuki, Trench-filled cellular parylene electret for piezoelectric transducer, *Appl. Phys. Lett.* **100**, 262901 (2012).
[140]Y. Feng and Y. Suzuki, All-polymer soft-X-ray-charged piezoelectret with embedded PEDOT electrode, *MEMS* (2013), pp. 865– 868.
[141]R. Gerhard, A matter of attraction: Electric charges localised on dielectric polymers enable electromechanical transduction, *Annual Reports IEEE Conf. Electrical Insulation and Dielectric Phenomena* (2014), pp. 1–10.
[142]X. Qiu, Ferroelectrets: Heterogenous polymer electrets with high electromechanical response, Habilitation thesis, University of Potsdam (2017).

[143]J. Wang, H. Liang, W. Fang and Y. Su, Composite rubber electret with piezoelectric 31 and 33 modes for elastically electromechanical sensors, *IEEE Sens.* (2015), doi:10.1109/ICSENS.2015.7370287.
[144]X. Zhang, P. Pondrom, L. Wu and G. M. Sessler, Vibration-based energy harvesting with piezoelectrets having high d31 activity, *Appl. Phys. Lett.* **108**, 193903 (2016).
[145]X. Zhang, P. Pondrom, G. M. Sessler and X. Ma, Ferroelectret nanogenerator with large transverse piezoelectric activity, *Nano Energy* **50**, 52 (2018).
[146]X. Qiu, W. Wirges and R. Gerhard, Polarization and hysteresis in tubular-channel fluoroethylenepropylene-copolymer ferroelectrets, *Ferroelectrics* **472** (1), 100 (2014).
[147]R. Gerhard, S. Bauer and X. Qiu, Charge-spring model for predicting the piezoelectric response of dielectric materials: Considering tetragonality extends validity to ferroelectric perovskites, *Annual Reports IEEE Conf. Electrical Insulation and Dielectric Phenomena* (2016), pp. 81–84.
[148]M. Wegener, W. Wirges, R. Gerhard-Multhaupt, M. Dansachmüller, R. Schwödiauer, S. BauerGogonea, S. Bauer, M. Paajanen, H. Minkkinen and J. Raukola, Controlled inflation of voids in cellular polymer ferroelectrets: Optimizing electromechanical transducer properties, *Appl. Phys. Lett.* **84**, 392 (2004).
[149]X. Qiu, Z. Xia and F. Wang, Influence of heat treatment temperature after the pressure expansion on the electromechanical properties of cellular polypropylene electret, *Acta Phys. Sin.* **55**(5), 2578 (2006)
[150]X. Qiu, F. Groth, W. Wirges and R. Gerhard, Cellular polypropylene foam films as DC voltage insulation and as piezoelectrets—A comparison, *IEEE Trans. Dielectr. Electr. Insul.* **25**(3), 829 (2018).
[151]E. Tuncer and M. Wegener, Elastic properties of highly anisotropic thin poly(propylene) foams, *Mater. Lett.* **58**, 2815 (2004).
[152]E. Tuncer, M. Wegener and R. Gerhard-Multhaupt, Modeling electro-mechanical properties of layered electrets: Application of the finite-element method, *J. Electrostat.* **63**, 21 (2005).
[153]R. A. P. Altafim, W. Wirges, X. Qiu, R. Gerhard, H. C. Basso, R. A. C. Altafim, W. Jenninger and J. Wagner, Dielectric resonance spectroscopy of piezoelectrets with tubular channels: Channel dimensions control resonances, *Proc. Int. Conf. Solid Dielectric* (2010).
[154]R. A. P. Altafim, R. A. C. Altafim, X. Qiu, S. Raabe, W. Wirges, H. C. Basso and R. Gerhard, Fluoropolymer piezoelectrets with tubular channels: Resonance behavior controlled by channel geometry, *Appl. Phys. A Mater.* **107**, 965 (2012).
[155]R. A. P. Altafim, X. Qiu, W. Wirges, R. A. C. Altafim, H. C. Basso, R. Gerhard, D. L. Chinaglia, W. Jenninger and J. Wagner, Template-based fluoropolymer ferroelectrets with multiple layers of tubular channels, *Annual Reports IEEE Conf. Electrical Insulation and Dielectric Phenomena* (2010).
[156]R. A. P. Altafim, R. A. C. Altafim, H. C. Basso, X. Qiu, W. Wirges and R. Gerhard, Fluoroethylenepropylene ferroelectrets with superimposed multi-layer tubular void channels, *Annual Reports IEEE Conf. Electrical Insulation and Dielectric Phenomena* (2011).
[157]G. C. Montanari, D. Fabiani, F. Ciani, A. Motori, M. Paajanen, R. Gerhard-Multhaupt and M. Wegener, Charging properties and time-temperature stability of innovative polymeric cellular ferroelectrets, *IEEE Trans. Dielectr. Electr. Insul.* **14**, 238 (2007).
[158]D. M. Taylor and O. Fernández, Thermal instability of electromechanical films of cellular polypropylene, *IEEE Trans. Dielectr. Electr. Insul.* **12**(4), 768 (2005).
[159]A. Mellinger, F. Camacho González and R. Gerhard-Multhaupt, Ultraviolet-induced discharge currents and reduction of piezoelectric coefficient in cellular polypropylene films, *Appl. Phys. Lett.* **82**, 254 (2003).
[160]D. Rychkov, A. Kuznetsov and A. Rychkov, Electret properties of polyethylene and polytetrafluoroethylene films with chemically modified surface, *IEEE Trans. Dielectr. Electr. Insul.* **18**, 8 (2011).
[161]D. Rychkov and R. Gerhard, Stabilization of positive charge on polytetrafluoroethylene electret films treated with titaniumtetrachloride vapor, *Appl. Phys. Lett.* **98**, 122901 (2011).
[162]D. Rychkov, R. Gerhard, V. Ivanov, A. Rychkov, Enhanced electret charge stability on polyethylene films treated with titaniumtetrachloride vapor, *IEEE Trans. Dielectr. Electr. Insul.* **19**(4), 1305 (2012).
[163]D. Rychkov, M. Yablokov and A. Rychkov, Chemical and physical surface modification of PTFE films — an approach to produce stable electrets, *Appl. Phys. A Mater.* **107**, 589 (2012).
[164]D. Rychkov, A. Rychkov, N. Efimov, A. Malygin and R. Gerhard, Higher stabilities of positive and negative charge on tetrafluoroethylene-hexafluoropropylene copolymer (FEP) electrets treated with titanium-tetrachloride vapor, *Appl. Phys. A Mater.* **112**(2), 283 (2013).
[165]D. Rychkov, R. Gerhard, A. Kuznetsov and A. Rychkov, Influence of charge density on the trap-energy spectrum in fluoroethylene-propylene copolymer films with chemically modified surfaces, *IEEE Trans. Dielectr. Electr. Insul.* **25**(3), 840 (2018).
[166]J. Wang, D. Rychkov and R. Gerhard, Chemical modification with orthophosphoric acid enhances surface-charge stability on polypropylene electrets, *Appl. Phys. Lett.* **110**(19), 192901 (2017)
[167]J. Wang, D. Rychkov, Q. Nguyen and R. Gerhard, The influence of orthophosphoric-acid surface modification on charge-storage enhancement in polypropylene electrets, *J. Appl. Phys.* **128**, 034102 (2020).
[168]Z. An, M. Zhao, J. Yao, Y. Zhang and Z. Xia, Influence of fluorination on piezoelectric properties of cellular polypropylene ferroelectrets, *J. Phys. D Appl. Phys.* **42**, 015418 (2009).
[169]Z. An, M. Mao, J. Cang, Y. Zhang and F. Zheng, Significantly improved piezoelectric thermal stability of cellular polypropylene films by high pressure fluorination and post-treatments, *J. Appl. Phys.* **111**, 024111 (2012).
[170]D. Rychkov, R. A. P. Altafim, X. Qiu and R. Gerhard, Treatment with orthophosphoric acid enhances the thermal stability of the piezoelectricity in low-density polyethylene ferroelectrets, *J. Appl. Phys.* **111**, 124105 (2012).
[171]D. Rychkov and R. A. P. Altafim, Template-based fluoroethylene-propylene ferroelectrets with enhanced thermal stability of piezoelectricity, *J. Appl. Phys.* **124**, 174105 (2018).
[172]Y. Xue, S. Li, M. Zhang, Z. Ruan, K. Wu, J. Cao, G. Li, X. Zhang and P. Fang, Air-borne ultrasonic transducers based on cross-linked polypropylene ferro/piezoelectrets, *IEEE Sens. J.* **22**(15), 14806–14814 (2022).
[173]P. Fang, L. Tian, Y. Zheng, J. Huang and G. Li, Using thin-film piezoelectret to detect tactile and slip signals for restoring sensation of prosthetic hands, *Conf. Proc. IEEE Engineering in Medicine and Biology Society* (2014), pp. 2565–2568.
[174]Q. Zhuo, L. Tian, P. Fang, G. Li and X. Zhang, A piezoelectret-based approach for touching and slipping detection in robotic hands, *2015 IEEE Int. Conf. Cyber Technology in Automation, Control, and Intelligent Systems (CYBER)* (2015), pp. 918–921.
[175]X. Ma, X. Zhang and P. Fang, Flexible film-transducers based on polypropylene piezoelectrets: Fabrication, properties, and applications in wearable devices, *Sensor. Actuat. A Phys.* **256**, 35 (2017).
[176]P. Fang, X. Ma, X. Li, X. Qiu, R. Gerhard, X. Zhang and G. Li, Fabrication, structure characterization, and performance testing of piezoelectret-film sensors for recording body motion, *IEEE Sens. J.* **18**(1), 401 (2018).
[177]X. Li, Y. Zheng, Y. Liu, L. Tian, P. Fang, J. Cao and G. Li, A novel motion recognition method based on force-myography of dynamic muscle contractions, *Front. Neurosci.* **15**, 783539 (2022).

[178]N. Wu, X. Cheng, Q. Zhong, J. Zhong, W. Li, B. Wang, B. Hu and J. Zhou, Cellular polypropylene piezoelectret for human body energy harvesting and health monitoring, *Adv. Funct. Mater.* **25**, 4788 (2015).
[179]Y. Chu, J. Zhong, H. Liu, Y. Ma, N. Liu, Y. Song, J. Liang, Z. Shao, Y. Sun, Y. Dong, X. Wang and L. Lin, Human pulse diagnosis for medical assessments using a wearable piezoelectret sensing system, *Adv. Funct. Mater.* **28**, 1803413 (2018).
[180]J. Nie, M. Ji, Y. Chu, X. Meng, Y. Wang, J. Zhong and L. Lin, Human pulses reveal health conditions by a piezoelectret sensor via the approximate entropy analysis, *Nano Energy* **58**, 528 (2019).
[181]P. Fang, Y. Peng, W. Lin, Y. Wang, S. Wang, X. Zhang, K. Wu and G. Li, Wrist pulse recording with a wearable piezoresistorpiezoelectret compound sensing system and its applications in health monitoring, *IEEE Sens. J.* **21**(18), 20921 (2021).
[182]W. Wirges, S. Raabe and X. Qiu, Dielectric elastomer and ferroelectret films combined in a single device: How do they reinforce each other? *Appl. Phys. A Mater.* **107**, 583 (2012).
[183]G. Kofod, M. Paajanen and S. Bauer, Self-organized minimumenergy structures for dielectric elastomer actuators, *Appl. Phys. A Mater.* **85**, 141 (2006).
[184]B. O'Brien, T. McKay, E. Calius, S. Xie and I. Anderson, Finite element modelling of dielectric elastomer minimum energy structures, *Appl. Phys. A Mater.* **94**, 507 (2009).
[185]G. Kofod, W. Wirges, M. Paajanen and S. Bauer, Energy minimization for selforganized structure formation and actuation, *Appl. Phys. Lett.* **90**, 081916 (2007).
[186]H. Kodama, Y. Yasuno, T. Miyata, K. Hiyama, K. Suzuki, H. Koike and S. Iida, Piezo-electret vibration sensors designed for acoustic-electric guitars, *IEEE Trans. Dielectr. Electr. Insul.* **27**(5), 1675 (2020).
[187]G. Gidion and R. Gerhard, The bow on a string: Bow vibrations detected with ferroelectret sensors, *Acta Acust. United Ac.* **104** (2), 315 (2018).
[188]Y. Gutnik, R. A. P. Altafim, P. R. Veronese, J. F. Resende, H. C. Basso, R. Gerhard and R. A. C. Altafim, Piezoelectret sensors detect geometry-related modifications of the acoustical signatures from partial discharges in an electrical equipment chamber, *Annual Reports IEEE Conf. Electrical Insulation and Dielectric Phenomena* (2012), pp. 108–111.